



A Comparison of Three Different Methods for the Identification of Hysterically Degrading Structures Using BWBN Model

Ying Zhao¹, Mohammad Noori^{1,2*}, Wael A. Altabey^{1,3,4} and Taher Awad⁴

¹ International Institute for Urban Systems Engineering, Southeast University, Nanjing, China, ² Department of Mechanical Engineering, California Polytechnic State University, San Luis Obispo, CA, United States, ³ Nanjing Zhixing Information Technology Company, Nanjing, China, ⁴ Department of Mechanical Engineering, Faculty of Engineering, Alexandria University, Alexandria, Egypt

OPEN ACCESS

Edited by:

Vagelis Plevis,
OsloMet – Oslo Metropolitan
University, Norway

Reviewed by:

Aristotelis E. Charalampakis,
National Technical University of
Athens, Greece
Eleni N. Chatzi,
ETH Zürich, Switzerland

*Correspondence:

Mohammad Noori
mnoori@outlook.com

Specialty section:

This article was submitted to
Computational Methods in Structural
Engineering,
a section of the journal
Frontiers in Built Environment

Received: 16 October 2018

Accepted: 11 December 2018

Published: 07 January 2019

Citation:

Zhao Y, Noori M, Altabey WA and
Awad T (2019) A Comparison of Three
Different Methods for the Identification
of Hysterically Degrading Structures
Using BWBN Model.
Front. Built Environ. 4:80.
doi: 10.3389/fbuil.2018.00080

Structural control and health monitoring scheme play key roles not only in enhancing the safety and reliability of infrastructure systems when they are subjected to natural disasters, such as earthquakes, high winds, and sea waves, but it also optimally minimize the life cycle cost and maximize the whole performance through the full life cycle design. In this scheme, system identification is regarded as a major technique to identify system states and related parameter variables, thus preventing degradation of structural or mechanical systems when unexpected disturbances occur. In this paper, three different strategies are proposed to identify general hysteretic behavior of a typical shear structure subjected to external excitations. Different case studies are presented to analyze the dynamic responses of a time varying shear structural system with the early version of Bouc-Wen-Baber-Noori (BWBN) hysteresis model. By incorporating a “Gray Box” strategy utilizing an Intelligent Parameter Varying (IPV) and Artificial Neural Network (ANN) approach, a Genetic algorithm (GA), and a Transitional Markov Chain Monte Carlo (TMCMC) based Bayesian Updating framework system identification schemes are developed to identify the hysteretic behavior of the structural system. Hysteresis characteristics, computational accuracy, and algorithm efficiency are further discussed by evaluating the system identification results. Results show that IPV performs superior computational efficiency and system identification accuracy over GA and TMCMC approaches.

Keywords: hysteretic behavior, BWBN model, Intelligent Parameter Varying (IPV), Genetic algorithm (GA), Transitional Markov Chain Monte Carlo simulation (TMCMC), Bayesian updating

INTRODUCTION

In recent years, an increasing attention is witnessed to face the challenging issues of safety, serviceability, reliability, risk and life-cycle management, and performance improvement of structures and infrastructure due to changing and more frequently occurring natural and man-made hazards, infrastructure crisis, and sustainability issues. These disturbances are dealt with innovative technologies to enhance structural functionality and safety in various stages of research and development (Spencer, 2003; Altabey, 2017a). Several types of structures that employ control

strategies for different application scopes can be found in Constantinou et al. (1998), Soong and Spencer (2002), and Altabay (2014, 2017b,c); Altabay (2018). Proper modeling of inherent non-linearity in vast majority of structural systems plays an important role in understanding structural response under hazardous loadings. System identification is an important approach in control strategy regarded as the interface between the mathematical world of control theory and the real world of application and model abstractions (Zadeh, 1956; Ljung, 2010; Altabay, 2016, 2017d,e; Altabay and Noori, 2017a, 2018; Zhao et al., 2018), and it handles a wide range of system dynamics problem without the prior knowledge of actual system physics. The schematic diagram of system identification process is depicted in **Figure 1**.

Hysteresis can be described as the hereditary and memory nature of a non-linear or inelastic system behavior where the restoring force is dependent on both instantaneous as well as past history of deformations. In general, under cyclic loading, mechanical and structural systems are capable of dissipating considerable energy and they exhibit appreciable hysteretic behavior with hysteresis loops. Each loop enclosing the area in the restoring force vs. displacement curve depicts the energy dissipated over a complete cycle resulting from internal friction within the structural system.

Various empirical hysteresis models have been proposed in the past few decades. A class of smoothly varying hysteresis models used in engineering fields are Bouc-Wen class of hysteresis models. Bouc suggested a smooth and versatile hysteresis model for non-linear systems and hysteretic systems (Bouc, 1967; Wen, 1975, 1976, 1980, 1986, 1989; Park et al., 1986; Wen and Yeh, 1989; Ikhouane and Rodellar, 2007; Ikhouane et al., 2007; Ikhouane and Gomis-Bellmunt, 2008). Baber and Wen extended the Bouc model to take the degradation in strength or stiffness of structural systems into account (Baber and

Wen, 1980). Baber-Noori, and later Noori, further extended the capabilities of Bouc-Wen model by including pinching behavior and studied the response of these systems under random excitation (Noori, 1984; Baber and Noori, 1986). Baber-Noori and subsequently Noori-Baber's work on integrating the pinching phenomenon in hysteretic behavior and extending Bouc-Wen-Baber (BWB) model was the first work in developing a smooth hysteresis model capable of taking into account strength and stiffness degradation as well as shear pinching phenomenon (Baber and Noori, 1985). BWBN was incorporated in structural design software, OpenSees developed at the University of California Berkeley (Hossain, 1995). A toolbox for computing the parameters of BWBN hysteresis model using multi-objective optimization evolutionary algorithms was also developed by SourceForge, an Open Source community (*Bouc Wen Baber Noori Model of Hysteresis, Source Forge*). Foliente showed Bouc-Wen-Baber-Noori (BWBN) model could produce previously observed inelastic behavior of wood joints and structural systems using BWBN smooth hysteresis model (Foliente, 1995; Zhao et al., 2017a,b; Noori et al., 2018). Deb et al. developed a toolbox that identifies structural parameters of Bouc-Wen-Baber-Noori hysteresis model through a novel multi-objective optimization evolutionary algorithms (MOBEAs) (Deb et al., 2002; Deb, 2013). Ortiz et al. analyzed and identified BWBN model via a multi-objective optimization algorithm (Ortiz et al., 2013). Peng et al. utilized BWBN model for identifying the parameters of a magneto-rheological damper and depicts its force-lag phenomenon (Peng et al., 2014). Muller et al. investigated the application of BWBN in their work and conducted performance-based seismic design through a Search-Based Cost Optimization (Muller et al., 2012). Chan et al. made a prediction of the hysteretic behavior of passive control systems by applying BWBN in a nonlinear-autoregressive-exogenous model (Chan et al., 2015).

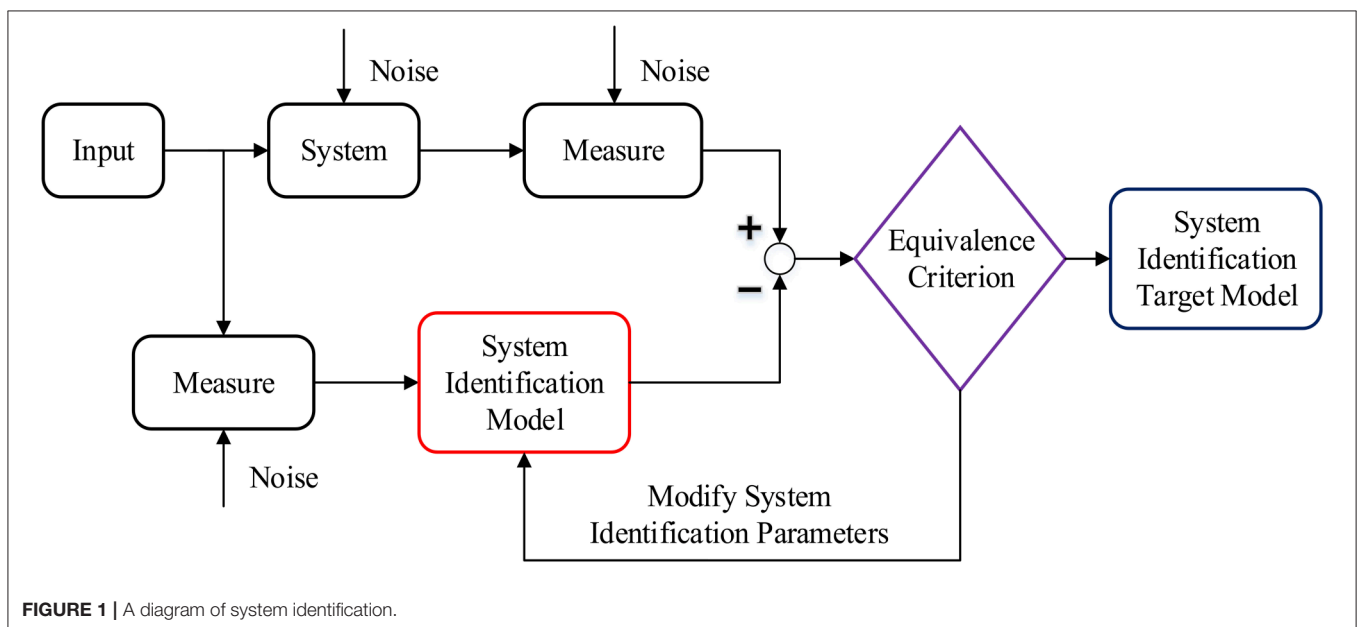


FIGURE 1 | A diagram of system identification.

Traditional artificial neural networks technique shows its superiority in the identification, monitoring, and control of complicated and non-linear dynamic systems (Narendra and Parthasarathy, 1990; Masri et al., 1992; Lu and Basar, 1998; Abouelwafa et al., 2014; Altabay and Noori, 2017b). However, a priori knowledge of the characteristics of restoring force is necessary and important for traditional parametric system identification approaches, while the non-parametric methods do not need information beforehand, lacking direct association between system dynamics and system model. In order to overcome the limitations of conventional parametric and non-parametric approaches, a novel Intelligent Parameter Varying (IPV) method was proposed, which makes full use of the embedded radial basis function networks to make an estimation of the hysteretic and inelastic characteristics of restoring forces constitutively for a multi degree of freedom system. A scaled three story base excited structure was designed to experimentally verify the non-linearity and its associated hysteresis of a structure using a displacement controlled shaking table (Saadat et al., 2003, 2004a,b, 2007). Further, a data-driven identification strategy for non-linear and hysteretic behaviors of steel wire strands was compared and verified using polynomial basis functions and neural networks. The results showed that neural networks were found more promising for the prediction of slightly pinched, hardening hysteresis, strongly pinched, hardening hysteresis, and classical quasi-linear softening hysteresis (Brewick et al., 2016). Genetic algorithms have been used for system identification of non-linear and hysteretic systems. The application of Real Coded Genetic Algorithms (RCGA) was demonstrated and applied to fit curves of synthetic and experimentally obtained Bouc-Wen hysteresis loops for a sandwich composite material (Hornig and Flowers, 2005). Different real coded genetic algorithms and their related criteria for efficiently identifying non-linear systems are regarded as non-classical and optimized identification techniques (Monti et al., 2009). A Bayesian probabilistic framework was proposed to detect damage of continuous monitored structures by incorporating load-dependent Ritz vectors as an alternative to modal vectors (Sohn, 1998). A large body of work was conducted to track, estimate and identify structural parameters, system status and hysteretic and degrading behavior of structures using Kalman filters, extended Kalman filters and unscented Kalman filters (Jeen-Shang and Yigong, 1994; Yang et al., 2006; Wu and Smyth, 2007, 2008; Chatzi and Smyth, 2009; Chatzi et al., 2010; Lei and Jiang, 2011; Mu et al., 2013; Kontoroupi and Smyth, 2017; Erazo and Nagarajaiah, 2018). Traditional Markov Chain Monte Carlo approach in conjunction with Bayesian updating method were applied for structural response predictions and performance reliability evaluation (Yuen and Katafygiotis, 2001; Zhang and Cho, 2001; Beck and Au, 2002). Later, a transitional Markov Chain Monte Carlo (TMCMC) approach was developed by designing optimized sampling strategy from a series of intermediate probability density functions (PDFs) that converge to the target PDF, thus avoiding sampling difficulties. The TMCMC theory and algorithm were verified and demonstrated through the performance of the developed sampling approach, different PDFs as well as higher dimensional problems (Ching and Chen, 2007; Muto, 2007; Muto and Beck, 2008; Worden and

Hensman, 2012; Zheng and Yu, 2013; Behmanesh and Moaveni, 2014; Green, 2015; Green et al., 2015; Ortiz et al., 2015).

It is a major barrier to successfully design hysteretic structures against degradation under severe cyclic loading. Most structural systems degrade with significant hysteresis, for example wood structures, dams, highways, reinforced concrete towers, steel bridges are critical and key elements of our built environment. In spite of their obvious importance, and their huge rehabilitation and replacement costs, design, construction, and analysis of the majority of these structures requires overly simplistic or in some cases flawed assumptions regarding hysteretic evolution. Development of a practical structural degrading identification approaches is much deserving. A comparative study of online and offline identification strategies for UAVs were discussed, and it is found that online approach is more adaptive to changes but with lower prediction accuracy (Puttige and Anavatti, 2007). Therefore, offline learning is employed in this paper. Based on what was discussed in the introduction above, the main contributions of the research are to present a three story hysterically degrading shear structure by incorporating BWBN slip lock hysteresis to represent the hysteretic restoring forces in this system. This BWBN model will be capable of producing all significant and prominent features of structural strength and stiffness degradations as well as slip lock behavior, and conduct a comparative study using three system identification approaches including an Intelligent Parameter Varying Artificial Neural Network developed in an earlier research work by a group that involved one of the authors (a “gray box” model that considers linear as well as non-linear parts of the dynamic system), genetic algorithm optimization method, and a novel TMCMC statistical approach.

The comparative study of the aforementioned approaches for system identification and their application in a structural system using *BWBN MODEL* is an original work. To the best of the authors’ knowledge such comparative study has not been reported in the literature.

STRUCTURAL SYSTEM MODELING AND SYSTEM IDENTIFICATION

BWBN Hysteresis Model

The model employed herein is an earlier version of BWBN hysteresis degradation model, which incorporates the previous smooth system degrading element by Bouc as modified by Baber and Wen in series with a slip-lock element (a non-linear hardening spring) developed by Baber and Noori. Under cyclic excitation, degradation manifests itself in the evolution of progressively varying hysteresis loops. A non-linear system governed by Equation (1) is given with the incorporation of BWBN model.

$$m\ddot{x} + c\dot{x} + R = F(t) \quad (1)$$

$$R = \alpha kx + (1 - \alpha) kz \quad (2)$$

$$\dot{z} = \frac{A\dot{x}_1 - \nu [\beta |\dot{x}_1| |z|^{n-1} z + \gamma \dot{x}_1 |z|^n]}{\eta} \quad (3)$$

$$\dot{x}_2 = \sqrt{\frac{2}{\pi}} \frac{s}{\sigma} \exp\left[-\frac{z^2}{2\sigma^2}\right] \dot{z} \tag{4}$$

$$\dot{\varepsilon} = (1 - \alpha) k \dot{x} z \tag{5}$$

$$s = \delta_s \varepsilon \tag{6}$$

$$(x = x_1 + x_2) \tag{7}$$

where, parameters m , c , k are, respectively, the mass, damping, and stiffness coefficients, and parameters \ddot{x} , \dot{x} , x are quantities that describe the system acceleration, velocity and displacement, and R is the restoring force and $F(t)$ is the ambient excitation. Parameter α is the weighting value denoting the ratio of post-elastic to initial stiffness. Parameters A , β , and γ are basic hysteresis shape control parameters. Parameter z is the hysteretic displacement, and n is the degree of the sharpness of yield. Strength and stiffness degradation coefficients are, respectively denoted by $\nu(\delta_\nu)$ and $\eta(\delta_\eta)$. Parameters x_1 and x_2 are Bouc-Wen hysteretic system displacement and the additional displacement that considers slip-lock behavior. Parameter ε is the measure of the combined effect of duration and severity of the energy dissipated through hysteresis, σ is a measure of the sharpness of the peak of the hysteresis, and δ_s measures the slip magnitude. All 10 parameters are essential to produce the common features of hysteretic behavior. It would be very helpful if a small number of unspecified parameters for system identification can be reduced in that large numbers of parameters increase the uncertainty of convergence for updating parameters in search space. It was proved that the redundancy of specific hysteresis parameters can be eliminated through mathematical transformations in the parameter space devised to freeze them without affecting the system response (Ma et al., 2004; Charalampakis and Koumoussis, 2008a,b; Charalampakis and Dimou, 2010).

Structural System Modeling

Restoring force curves of reinforced or steel structures show complex hysteresis characteristics, revealing material non-linearity, crack opening and closing, bond and slip between steel bars and concrete and low cycle fatigue that result in structural strength and stiffness degradation. The hysteresis model used herein considers the specific case appropriate for both strength

and stiffness degradations, and slip-lock behavior of restoring hysteretic forces of the structure. All the restoring forces of the structure are assumed to follow the BWBN hysteresis model. The structural system considered in this study is a shear type model subjected to ambient sinusoidal wave and ElCentro seismic excitation as input signals \ddot{x}_g . The ground excitation motion \ddot{x}_g makes an integral transformation to be incorporated into the structural equations. The structural system mainly includes three lumped mass coupled subsystems, as shown in **Figure 2**. These masses are lumped at floor (floor m_i), levels and these floors are assumed and constrained to only move laterally. The restoring force R_i , in conjunction with the stiffness between the adjacent floors, are represented by dampers and springs, with the corresponding coefficients c_i and k_i , respectively. The time varying system yields energy dissipation due to the hysteretic behavior of the inner structure.

For this three story shear structure, the equations of motion are represented by Equations (8–10):

$$m_3 \ddot{x}_3 + c_3 (\dot{x}_3 - \dot{x}_2) + R_3 = 0 \tag{8}$$

$$m_2 \ddot{x}_2 + c_2 (\dot{x}_2 - \dot{x}_1) + R_2 - c_3 (\dot{x}_3 - \dot{x}_2) - R_3 = 0 \tag{9}$$

$$m_1 \ddot{x}_1 + c_1 (\dot{x}_1 - \dot{x}_g) + R_1 - c_2 (\dot{x}_2 - \dot{x}_1) - R_2 = 0 \tag{10}$$

System Identification Theory

A typical system identification framework mainly has two components including system itself and system identification model. By defining an equivalence criterion, the parameters of the system identification model are updated via a comparison with the original system, until the system identification model will be eventually equivalent to the original system. System identification approaches used in this paper include intelligent parameter varying based approach, GA based approach and transitional markov chain monte carlo (TMCMC) based approach. IPV approach employs ANNs and establishes a ‘‘Gray Box’’ system, where the original system parameters are replaced by the parameters of ANNs, and the system structure is replaced by ANNs. For GA and TMCMC methods, they are used to optimize and identify the parameters of system model, which is regarded as an approximate model of the original real system. The

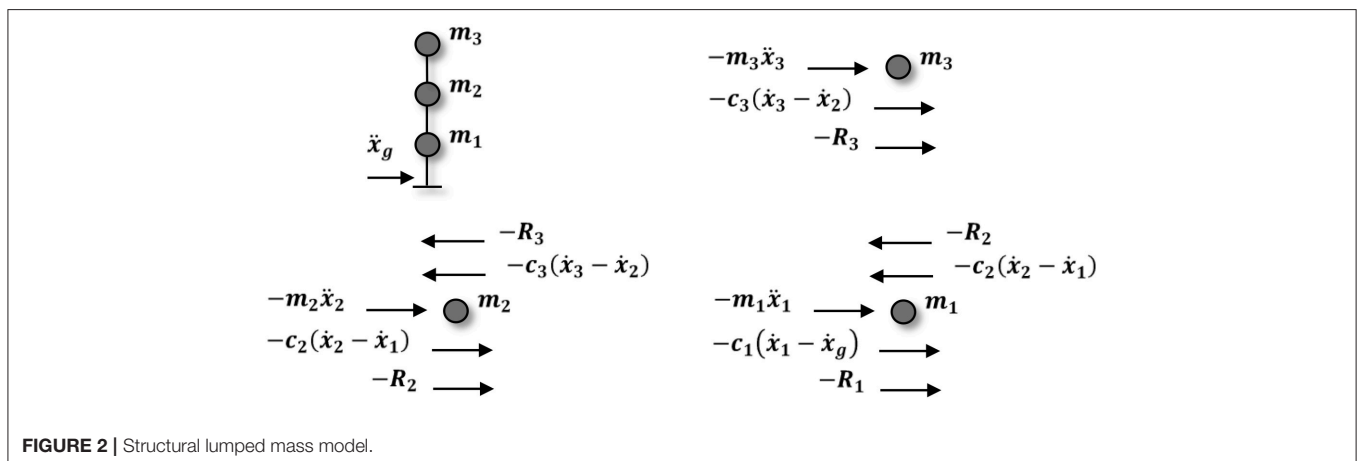


FIGURE 2 | Structural lumped mass model.

theoretical background for the three approaches are presented in the following subsections.

Intelligent Parameter Varying Based System Identification

Artificial neural network (ANN) is a non-linear and adaptive information processing system composed of large numbers of neuron units. A radial basis function (RBF) neural network is employed to build the intelligent parameter varying model. In ANN architecture, the Euclidean distance between the clustering center and input vector is calculated and the result is activated to pass through the output layer. The activation function is Gaussian output function and is formulated as:

$$g_j = \exp\left(-\frac{\sum_{i=1}^n (x_i - c_j)^2}{\sigma_j^2}\right) \quad (11)$$

where g_j is the output of the j^{th} unit in the hidden layer, x_i is the input data fed to the network, c_j is the center of the j^{th} unit in the input space, and σ_j is the width of the j^{th} function. $j = 1, 2, \dots, m$. Parameter m is the number of the centers of neurons, and n represents the dimension of the input space. Linearly weighted summation of hidden layer node outputs produces the output nodes. Therefore, the output of the network is calculated by:

$$y = \sum_{j=1}^n w_j g_j \quad (12)$$

where w_j is the weight of the j^{th} node.

The objective is to find a series of weights that minimize the square of error between the actual and desired network outputs, i.e.,:

$$E(k) = \frac{1}{2} \sum_{j=1}^N (d(k) - y(k))^2 \quad (13)$$

where $d(k)$ is the desired output and $y(k)$ the actual output of RBF and $j = 1, 2, \dots, N$, and N is the number of data sets. There are commonly two approaches for utilizing ANNs, i.e., supervised and unsupervised learning. In supervised approach the input and the referred output are usually known. The network then processes the input values and makes a comparison between its resulting output and the desired output. The network system makes the errors propagate back through different layers, causing the system to adjust tuned weights which control the network. This process repeats over and over until all the weights are continually tweaked in an appropriate way. During the training process of a network the connection weights are continually refined to a specific generalization level and a good network performance level. In unsupervised training, the system itself must then decide what features and how many features need to be extracted to group the input data, which is often referred to as self-organization or adaption. Herein, we use the non-supervised learning algorithm to acquire the centers and variance of radial

basis function, and meanwhile the least mean squared error is acquired by using supervised learning algorithm. The response of the hysteretic system is used as the desired signal, and the error between the desired signal and the simulated signal is back propagated to modify the weights and threshold values of neural network model.

Parametric system identification approaches have been widely used but in most published literature in this area a priori knowledge of the characteristics depicting the behavior of restoring force is required. Non-parametric approaches generally do not need information beforehand but they typically lack direct associations between system dynamics and associated model. When ANNs are implemented using the “Black Box” approach, little of the system information might be obtained from the traditional techniques due to the fact that the “Black Box” only considers system input and output. Intelligent Parameter Varying (IPV) method preserves the benefits of both traditional parametric and non-parametric approaches, and utilizes the embedded radial basis function as the activation of neurons to estimate the constitutive characteristics of inelastic and hysteretic restoring forces for a multi degree of freedom structural system.

IPV technique, i.e., a gray box approach (**Figure 3**) that incorporates the advantages of both “White Box” and “Black Box” approaches, was developed in such a way that the model structure can be determined using the first principle (Equations 18–20), while non-linear and adaptive learning capabilities of ANNs can be used to identify the non-linear, time varying system’s dynamics (Equations 24–26) that would be difficult to model and identify using the traditional “White Box” and “Black Box” (Saadat et al., 2003, 2004a,b, 2007).

A non-linear system with full state measurement represented by the Linear Parameter Varying (LPV) model structure is given by:

$$\dot{x} = f_1(x, u) \cdot x + f_2(x, u) \cdot u \quad (14)$$

$$y = x \quad (15)$$

The IPV approach introduced herein would preserve the model structure inherent in Equation (14) without requiring a priori representations of non-linearities $f_1(x, u)$ and $f_2(x, u)$. Instead, these terms would be represented by separate artificial neural networks $g_1(x, u, w_1)$ and $g_2(x, u, w_2)$ as depicted in Equations (16, 17):

$$\dot{x} = g_1(x, u, w_1) \cdot x + g_2(x, u, w_2) \cdot u \quad (16)$$

$$y = x \quad (17)$$

By modeling the non-linearities $f_1(x, u)$ and $f_2(x, u)$ via separate artificial neural networks $g_1(x, u, w_1)$ and $g_2(x, u, w_2)$, the model structure (Equations 16, 17) is preserved. Therefore, the relationship between the model structure and artificial neural network parameters is preserved. The structural model is preserved by incorporating ANN, preserving a portion of information of the structural model. The IPV approach preserves the direct association between the construction of ANN and the system dynamics, used for structural health monitoring for system identification.

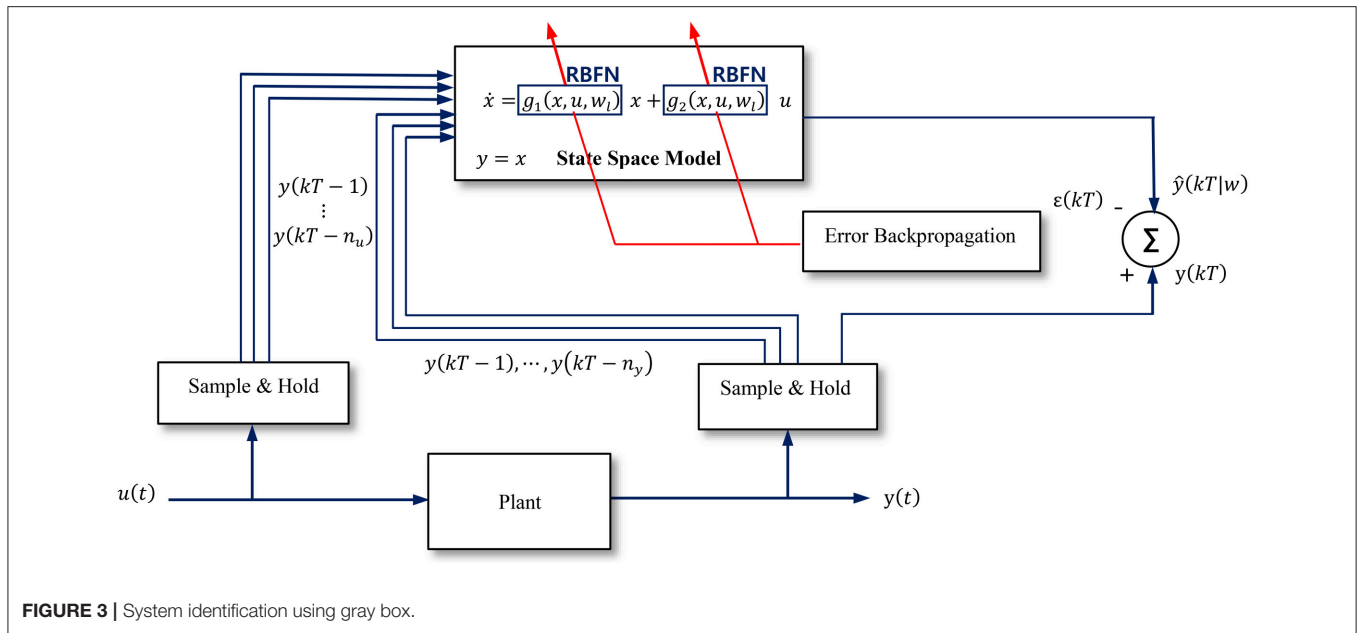


FIGURE 3 | System identification using gray box.

Based on first principle, system dynamics can be transformed to the following form:

$$-c_3(\dot{x}_3 - \dot{x}_2) - R_3 - m_3\ddot{x}_g = m_3\ddot{u}_3 \tag{18}$$

$$-c_2(\dot{x}_2 - \dot{x}_1) - R_2 + c_3(\dot{x}_3 - \dot{x}_2) + R_3 - m_2\ddot{x}_g = m_2\ddot{u}_2 \tag{19}$$

$$-c_1(\dot{x}_1 - \dot{x}_g) - R_1 + c_2(\dot{x}_2 - \dot{x}_1) + R_2 - m_1\ddot{x}_g = m_1\ddot{u}_1 \tag{20}$$

where u_1, u_2, u_3 , respectively represent the relative displacements of each floor, i.e., $u_1 = x_1 - x_g, u_2 = x_2 - x_g, u_3 = x_3 - x_g$.

$$-R_3 - m_3\ddot{x}_g = m_3\ddot{u}_3 \tag{21}$$

$$-R_2 + R_3 - m_2\ddot{x}_g = m_2\ddot{u}_2 \tag{22}$$

$$-R_1 + R_2 - m_1\ddot{x}_g = m_1\ddot{u}_1 \tag{23}$$

The stiffness and damping terms are lumped into restoring forces, since in the hysteresis models the restoring force R associates with the lateral relative displacement x_r and the restoring displacement z , where z is expressed by the function of lateral relative velocity \dot{x}_r .

The modeling for the restoring forces using radial basis function based neural network is as follows:

$$\hat{R}_3 = g_3(\ddot{u}_3, \ddot{x}_g) \tag{24}$$

$$\hat{R}_2 = g_2(\ddot{u}_2, \ddot{x}_g, \hat{R}_3) \tag{25}$$

$$\hat{R}_1 = g_1(\ddot{u}_1, \ddot{x}_g, \hat{R}_2) \tag{26}$$

where, $\hat{R}_1, \hat{R}_2, \hat{R}_3$ represent, respectively, the identified restoring forces through the training of ANN as shown in Figure 4.

Genetic Algorithm Based System Identification

Genetic algorithm (GA) is an approach that searches the global optimal solution by simulating a natural evolution process.

The objective function can be formulated as the normalized mean square error (MSE) of the predicted time history $\tilde{y}(t|p)$ as compared to the reference time history $y(t)$. Herein, the acceleration response signal is employed as the time history series. The purpose of the following optimization approach is to minimize the difference (or the error) between predicted time history and the referred time history. The hysteretic structural system objective function is introduced below:

$$OF(p) = \frac{\sum_{i=1}^n (y(t_i) - \tilde{y}(t_i|p))^2}{N\sigma_y^2} \tag{27}$$

where p is a parameter vector, σ_y^2 the variance of the reference history, and N the number of points used. Sum of three acceleration response signal differences of the hysteretic structural system is used as the objective function. The optimization problem can be stated as the minimization of the objective function $OF(p)$ when the parameter vector has the following side constraints as:

$$x_{LB} \leq p \leq x_{UB} \tag{28}$$

where x_{LB} and x_{UB} are vectors defining the lower and the upper values of the model parameters, respectively. The basic strategy for the parameter identification using GA is shown in Figure 5. GA operates starting from a population of the potential solutions to a representative problem, and one population is composed of numbers of individuals coded by genes. Each individual is chromosomes with the characteristics of entity. GA initializes on a population of individuals (coded candidate solutions to the problem) that are manipulated by some operators such as selection, crossover, and mutation. In short, the selection process drives the search direction toward the region of best individuals, and the cross operator combines individuals to generate offsprings.

If it is indispensable to make selection and crossover operators converge toward the optimum, mutation alters one or more gene values (individuals) in a chromosome from its initial state, thus, maintaining genetic diversity from one generation of a population to the next. In this way, a complete exploration of global search space is forced by algorithm within the search space. Each individual in the population is represented as chromosome, indicating the collection of parameters are supposed to identify. GA adopts an elitist strategy, which consists of the preservation of the most fit individuals obtained in the current generation. Population representation and initialization generate population and individuals, and the initialized value will be assigned to the parameter space for solving the hysteretic system model. The fitness function is established by using the prediction error between the simulated signal response and predicted signal response. After a series of successive mathematical operators for optimization, the next generational loop begins.

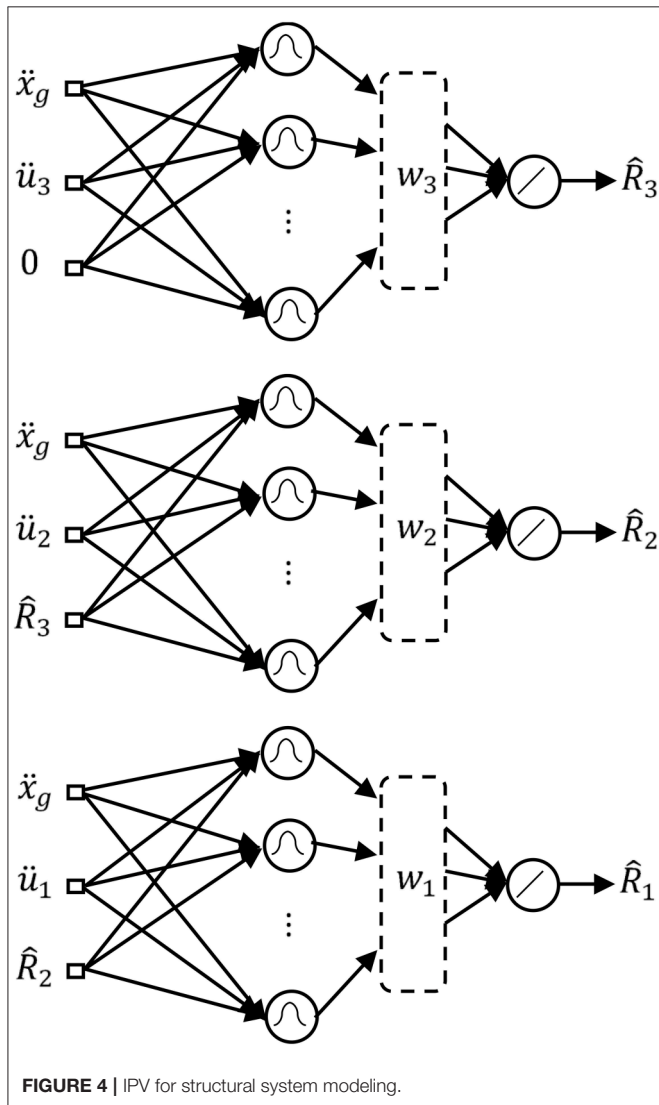


FIGURE 4 | IPV for structural system modeling.

Transitional Markov Chain Monte Carlo Based System Identification

Markov Chain Monte Carlo (MCMC) is an analytic approach which replaces numerical integration through summation over numbers of samples generated from iteration. A Markov chain is a stochastic process where one state is transformed to another state after a sufficiently long sequence of transition procedure. The next state is conditionally based on the last state. A key property of Markov chain is that the starting state has no influence on the state of the chain via a series of sequential transitions. The chain reaches its steady state at a specific point

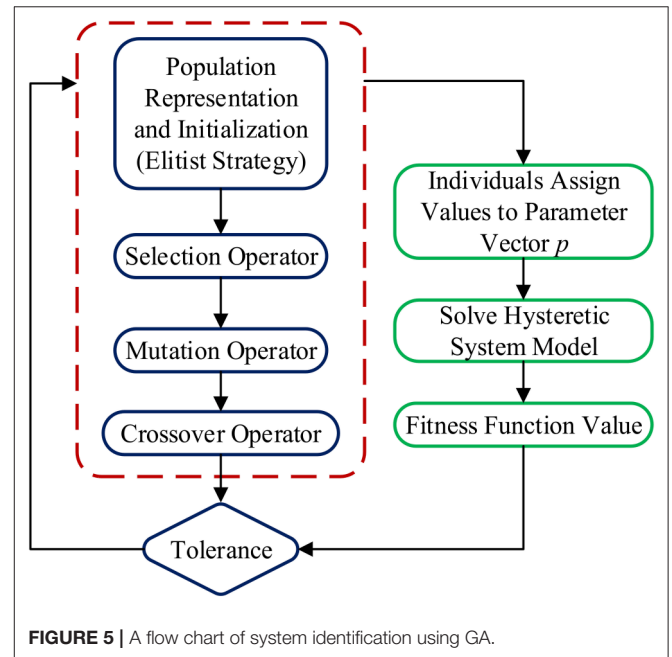


FIGURE 5 | A flow chart of system identification using GA.

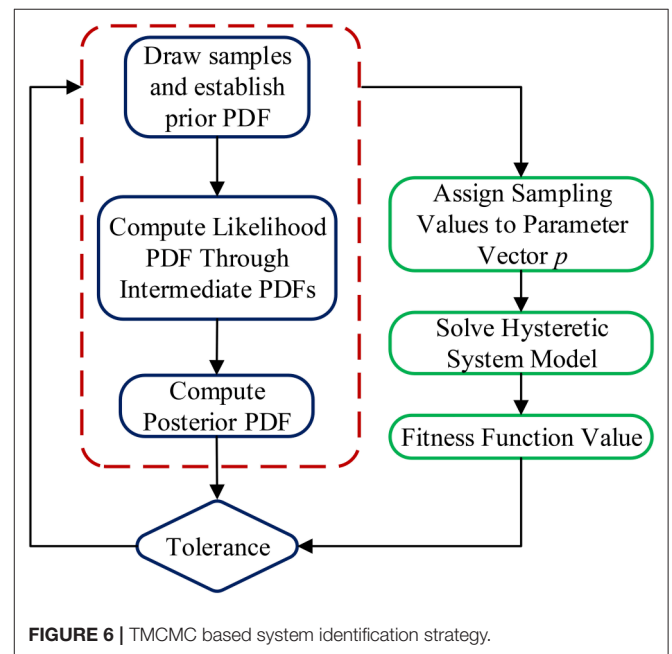


FIGURE 6 | TMCMC based system identification strategy.

where it reflects sampling distribution from stationary status. The principle of Monte Carlo simulation is applied for the integration to approximate the expected complex distribution status of numbers of samples. By increasing the number of samples, the approximation accuracy can be measured and achieve a desired value, which mainly depends on the independence of the samples.

Markov chain involves a stochastic sequential process where a series of states can be sampled from some stationary distributions while Monte Carlo sampling can make an estimation of various characteristics of a specific distribution. The goal of MCMC is to design a Markov chain to meet the target distribution of the chain which is what we are interested in sampling from.

Transitional Markov Chain Monte Carlo Theory (TMCMC) is introduced to avoid the difficulty of sampling from complicated target probability distributions (e.g., multimodal PDFs, PDFs with flat manifold, and very peaked PDFs) but sampling from a series of intermediate PDFs that converge to the target PDF and are easier to sample.

Bayesian Inference describes a process of solving posterior density functions given the likelihood and prior probability. The target probabilistic model can be depicted by M , D is the data acquired from the system, and the uncertain parameters of the model are described as θ . Sampling from the posterior PDF of θ conditioned on D is the aim of the Bayesian model updating, which is given as:

$$f(\theta|M, D) = \frac{f(D|M, \theta) \cdot f(\theta|M)}{f(D|M)} = \frac{f(D|M, \theta) \cdot f(\theta|M)}{\int f(D|M, \theta) \cdot f(\theta|M) \cdot d\theta} \quad (29)$$

where $f(\theta|M)$ is the prior PDF of θ , $f(D|M, \theta)$ is the likelihood of D given θ , and $f(D|M)$ is the evidence of the model M .

Bayesian model updating generally employs simulation based methods in that it is effective to obtain samples from $f(\theta|M, \theta)$, which can be estimated at a specific quantity of interest $E(g|M, D)$ based on the Law of Large Number.

$$E(g|M, D) \approx \frac{1}{N} \sum_{k=1}^N g(\theta_k) \quad (30)$$

where $\{\theta_k : k = 1, 2, \dots, N\}$ represents a set of N samples from $f(\theta|M, D)$. Consider the equation as follow:

$$f(\theta|M, D) \propto f(\theta|M) \cdot f(D|M, \theta) \quad (31)$$

It is usually difficult to sample from $f(\theta|M, D)$ using Importance Sampling (IS) and Metropolis–Hastings (MH) in that it is not so easy to understand the geometry of the likelihood $f(D|M, \theta)$. To converge to the target PDF $f(\theta|M, D)$ from the prior PDF $f(\theta|M)$, a series of intermediate PDFs are constructed as the following:

$$f_j(\theta) \propto f(\theta|M) \cdot f(D|M, \theta)^{p_j}, \quad j = 0, 1, \dots, m$$

$$0 = p_0 < p_1 < \dots < p_m = 1 \quad (32)$$

Note that $f_0(\theta) = f(\theta|M)$, $f_m(\theta) = f(\theta|M, D)$.

TABLE 1 | Parameter assignment for different cases.

Approach	Case	Parameter	m_1	m_2	m_3	k_1	k_2	k_3	c_1	c_2	c_3	A	α	β	γ	n	δ_v	δ_{v1}	δ_η	$\delta_{\eta1}$	σ	δ_s
IPV	Sin	-	1.0	1.0	1.0	10	10	10	0.05	0.05	0.05	1	0.01	2	2	1	0	1.5	0	1.5	0.01	0.05
	EiCentro	-	1.0	1.0	1.0	20	20	20	0.05	0.05	0.05	1	0.01	2	2	1	0	3	0	3	0.01	0.05
GA	Sin	True Value	1.0	1.0	1.0	10	10	10	0.05	0.05	0.05	1	0.01	2	2	1.5	0	1.5	0	1.5	0.01	0.05
		Lower bound	-	-	-	5	5	5	0.01	0.01	0.01	0.1	0.001	0.1	0.1	1	0	0.1	0	0.1	0.001	0.01
		Upper bound	-	-	-	15	15	15	0.1	0.1	0.1	2	0.02	4	4	2	0.1	3	0.1	3	0.02	0.1
	EiCentro	True Value	1.0	1.0	1.0	20	20	20	0.05	0.05	0.05	1	0.01	2	2	1.5	0	3	0	3	0.01	0.05
	Lower bound	-	-	-	15	15	15	0.01	0.01	0.01	0.1	0.001	0.1	0.1	1	0	0.1	0	0.1	0.001	0.01	
	Upper bound	-	-	-	25	25	25	0.1	0.1	0.1	2	0.02	4	4	2	0.1	6	0.1	6	0.02	0.1	
TMCMC	Sin	True Value	1.0	1.0	1.0	10	10	10	0.05	0.05	0.05	1	0.01	2	2	1.5	0	1.5	0	1.5	0.01	0.05
		Lower bound	-	-	-	5	5	5	0.01	0.01	0.01	0.1	0.001	0.1	0.1	1	0	0.1	0	0.1	0.001	0.01
		Upper bound	-	-	-	15	15	15	0.1	0.1	0.1	2	0.02	4	4	2	0.1	3	0.1	3	0.02	0.1
	EiCentro	True Value	1.0	1.0	1.0	20	20	20	0.05	0.05	0.05	1	0.01	2	2	1.5	0	3	0	3	0.01	0.05
	Lower bound	-	-	-	15	15	15	0.01	0.01	0.01	0.1	0.001	0.1	0.1	1	0	0.1	0	0.1	0.001	0.01	
	Upper bound	-	-	-	25	25	25	0.1	0.1	0.1	2	0.02	4	4	2	0.1	6	0.1	6	0.02	0.1	

In IPV approach, the number of hidden layer neurons is assigned 20, the initial weights are assigned with random values, and the minimum training speed is assigned 0.9.
 In GA approach, the population size is assigned 100, the elite count is 10, and crossover fraction is 0.6, and the generation is 30.
 In TMCMC approach, the sampling points are assigned 5000, and the scaling factor is assigned 0.2.

where the index j denotes the stage number. Although the geometry changing from $f(\theta|M)$ to $f(\theta|M, D)$ is large, the status of two changing adjacent intermediate PDFs is small. It is efficient to sample from $f_{j+1}(\theta)$ according to the previous sample from $f_j(\theta)$ through this small change.

The function $f_j(\theta)$ is used to extract samples and make an estimation of the PDF itself as a kernel density function (KDF), a combination of weighted Gaussian functions centered at the samples. The kernel density function can be regarded as the proposal PDF of the MH method to sample from $f_{j+1}(\theta)$. This will subsequently and ultimately result in $f(\theta|M, D)$ samples. This approach is called adaptive Metropolis–Hastings (AMH) algorithm. Given that the proposal PDF (KDF) function is fixed, rendering the MH method is as similar as IS, not efficient in high dimension situation.

It is a totally different strategy for TMCMC to acquire $f_{j+1}(\theta)$ samples based on $f_j(\theta)$ samples, KDF method is replaced by a resampling algorithm. It covers a battery of resampling stages, with each stage completing the following, given N_j samples from $f_j(\theta)$, depicted by $\{\theta_{j,k} : k = 1, \dots, N_j\}$, acquire samples from $f_{j+1}(\theta)$, depicted by $\{\theta_{j+1,k} : k = 1, \dots, N_{j+1}\}$. It can be calculated by the following in a more easier way, with the samples $\{\theta_{j,k} : k = 1, \dots, N_j\}$ from $f_j(\theta)$. The “plausibility weights ($w(\theta_{j,k})$)” of these samples regarding $f_{j+1}(\theta)$ can be computed by:

$$w(\theta_{j,k}) = \frac{f(\theta_{j,k}|M)f(D|M, \theta_{j,k})^{p_{j+1}}}{f(\theta_{j,k}|M)f(D|M, \theta_{j,k})^{p_j}} = f(D|M, \theta_{j,k})^{p_{j+1}-p_j}, \quad k = 1, \dots, N_j \quad (33)$$

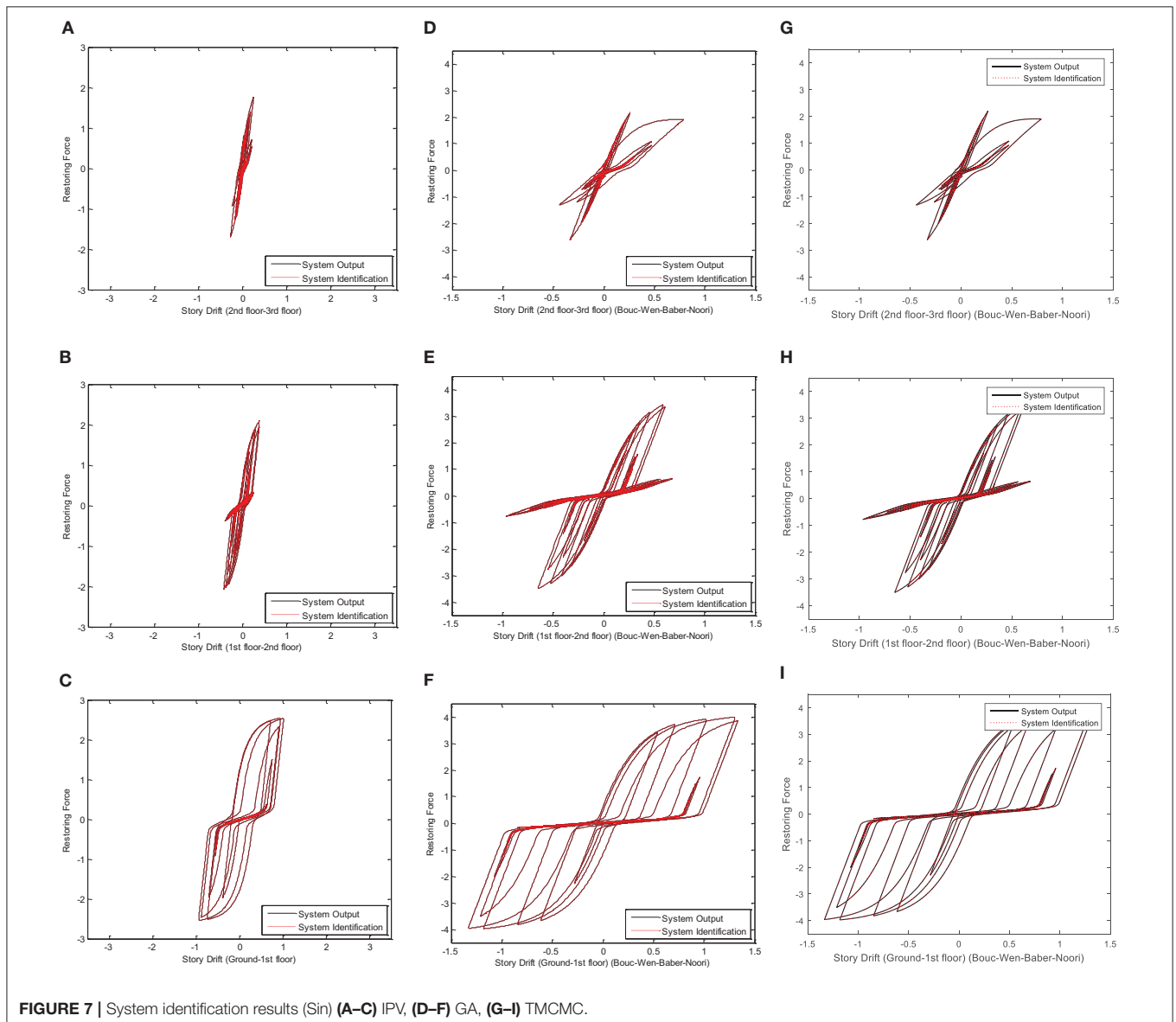


FIGURE 7 | System identification results (Sin) (A–C) IPV, (D–F) GA, (G–I) TMCMC.

Based on the normalized weights, the uncertain parameters can be resampled, i.e. let: $\theta_{j+1,k} = \theta_{j,l}$ and $w.p.$ $\frac{w(\theta_{j,l})}{\sum_{l=1}^{N_j} w(\theta_{j,l})}$ $k = 1, \dots, N_{j+1}$

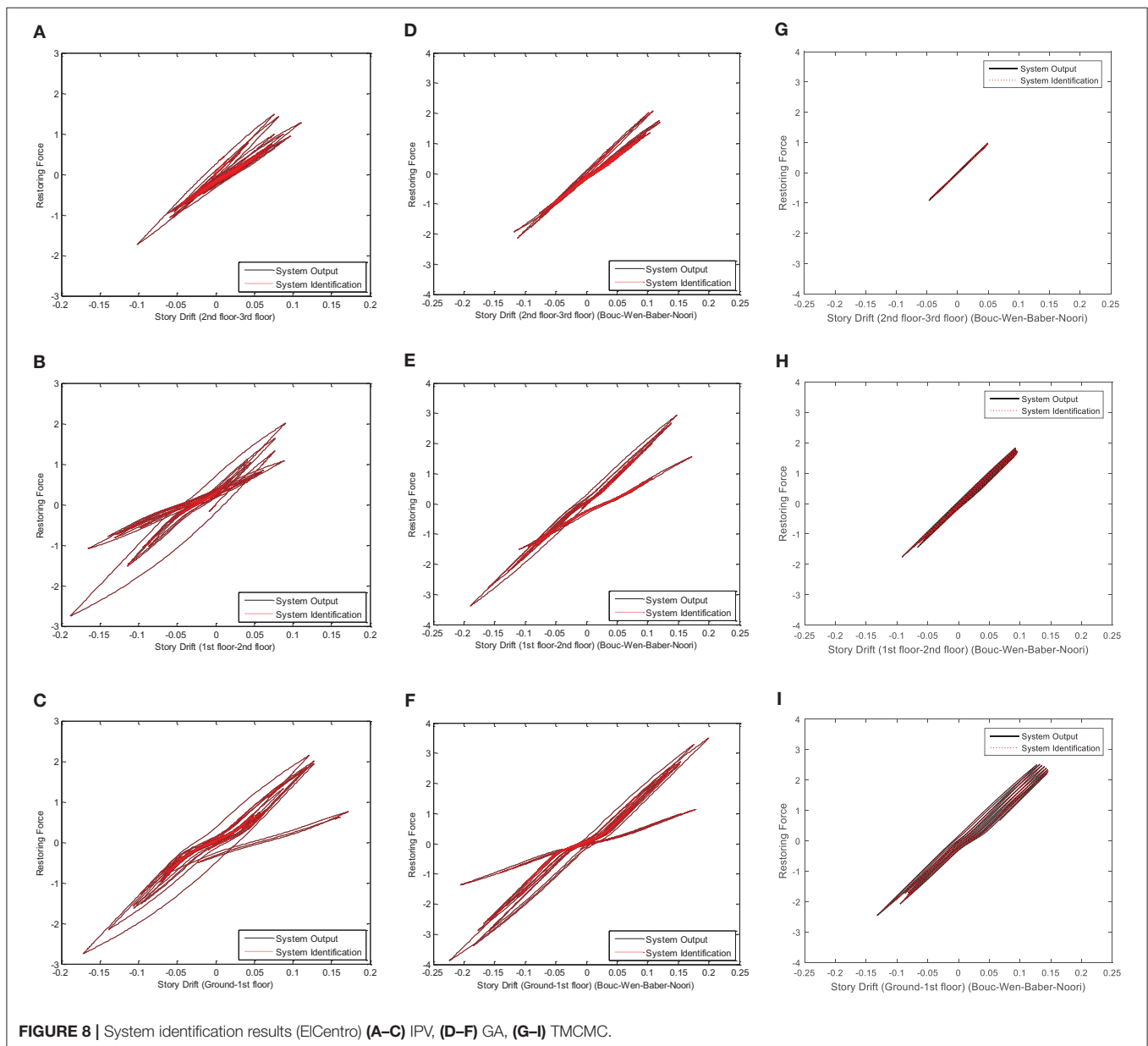
where “with probability” is represented by *w.p.* and pacifier index is denoted as *l*. It is shown that if N_j and N_{j+1} achieve a relatively large quantity, $\{\theta_{j+1,k} : k = 1, \dots, N_{j+1}\}$ will be distributed as $f_{j+1}(\theta)$. Moreover, $w(\theta_{j,k})$ is expected as the following value:

$$E[w(\theta_{j,k})] = \int w(\theta) \cdot f_j(\theta) \cdot d\theta = \int f(D|M, \theta)^{p_{j+1}-p_j} \cdot f_j(\theta) \cdot d\theta$$

$$= \int f(D|M, \theta)^{p_{j+1}-p_j} \cdot \frac{f(\theta|M)f(D|M, \theta)^{p_j}}{f(\theta|M)f(D|M, \theta)^{p_j}} \cdot d\theta = \frac{\int f(\theta|M)f(D|M, \theta)^{p_{j+1}} d\theta}{\int f(\theta|M)f(D|M, \theta)^{p_j} d\theta} \quad (34)$$

Therefore, $\sum_{k=1}^{N_j} w(\theta_{j,k})/N_j$ is the automatically unbiased estimation made for $\frac{\int f(\theta|M)f(D|M, \theta)^{p_{j+1}} d\theta}{\int f(\theta|M)f(D|M, \theta)^{p_j} d\theta}$. According to the results above, the following method is used to sample from $f(\theta|M, D)$ and make an estimation of $f(D|M)$.

More precisely, with probability $w(\theta_{j,k})/\sum_{l=1}^{N_j} w(\theta_{j,l})$, by using a covariance matrix equal to the scaled version of the estimated covariance matrix of $f_{j+1}(\theta)$, a Markov chain sample



in the k^{th} chain can be generated from a Gaussian proposal PDF centered at the current sample of the k^{th} chain:

$$\sum_j = \beta^2 \sum_{k=1}^{N_j} w(\theta_{j,k}) \left\{ \theta_{j,k} - \left[\frac{\sum_{l=1}^{N_j} w(\theta_{j,l}) \theta_{j,l}}{\sum_{l=1}^{N_j} w(\theta_{j,l})} \right] \right\} \times \left\{ \theta_{j,k} - \left[\frac{\sum_{l=1}^{N_j} w(\theta_{j,l}) \theta_{j,l}}{\sum_{l=1}^{N_j} w(\theta_{j,l})} \right] \right\}^T \quad (35)$$

where β is the prescribed scaling factor, $\sum_j = \text{product of } \beta^2$ and the estimated covariance of $f_{j+1}(\theta)$. The rejection rate is chosen as the value β , and MCMC may probably achieve a larger value accordingly. The value 0.2 is found to be more reasonable for the scaling parameter β .

It is essential to choose $\{p_j : j = 1, \dots, m - 1\}$. The larger value of p is desirable to make the transition between the intermediate adjacent PDFs smoother. The number of intermediate stages achieves a huge value if the increase of p -values has slow change rates.

The degree of uniformity of the plausibility weights $\{w(\theta_{j,k}) : k = 1, \dots, N_j\}$ can appropriately indicate how close $f_{j+1}(\theta)$ approaches $f_j(\theta)$, so p_{j+1} should be chosen so that the coefficient of variation (COV) of the plausibility weights can be equivalent to a prescribed threshold. The Bayesian inference framework for system identification is established (Figure 6) for structural model updating, which is regarded as a determinant reason for choosing the most suitable model parameters related to the hysteretic behavior of the structures by minimizing the difference between the predicted structural response and the simulated structural response. For the hysteretic structural model, the uncertain model parameters are selected as the ones that need to be updated through Bayesian inference (Equation 31) by drawing samples of parameters from the posterior PDF of parameters.

The TMCMC based Bayesian Updating algorithm is coded and implemented to establish the computational environment via exchange of data between the model and the algorithm. The evolution of parameter updating process is that, the samples from the prior PDFs are approximately uniformly distributed in the model parameter space at the first stage ($p_0 = 0$). Through applying Bayesian inference with TMCMC probabilistic simulations, the samples eventually populate well in the high probability region of the posterior PDFs close to the true model parameters at the last stage ($p_m = 1$).

TMCMC approach is employed to make an identification of the parameters of Bouc-Wen class models, henceforth represented by the vector $\theta \leq \Theta \subseteq R^d$. The appropriate choice of θ reflects the corresponding non-linear and hysteretic behavior of structure. By applying Bayesian model updating, the major advantage is that the result gives a probability distribution expressing the likelihood probability distribution of different parameters rather than yielding a single value for θ . It is clear that the evolution of the model parameter variation represents the Bayesian inference process.

TABLE 2 | Parameter identification error for different cases.

Approach	SNR	Case	k_1	k_2	k_3	c_1	c_2	c_3	A	α	β	γ	η	$\delta_{\eta 1}$	δ_{η}	δ_{p1}	δ_p	η	σ	δ_s	
GA	-	Sin	4.26%	-3.76%	-7.89%	-2.82%	1.00%	2.50%	2.05%	0.90%	0.78%	-3.10%	-2.77%	Inf	Inf	-2.04%	Inf	2.46%	-0.30%	-1.74%	
		EiCentro	-1.13%	0.41%	-1.41%	-0.44%	-0.88%	2.94%	1.07%	1.07%	4.20%	0.31%	0.39%	2.03%	Inf	Inf	0.43%	Inf	-2.86%	5.10%	0.80%
	30	Sin	3.78%	-2.82%	-6.63%	1.26%	1.94%	2.30%	2.30%	3.29%	-1.40%	-1.63%	0.04%	-4.73%	Inf	Inf	0.58%	Inf	4.42%	-4.60%	-0.96%
		EiCentro	-1.07%	0.60%	-0.79%	-0.48%	0.96%	2.30%	2.30%	0.65%	-2.90%	1.95%	-1.75%	2.86%	Inf	Inf	-0.97%	Inf	-1.61%	2.50%	-1.32%
	10	Sin	4.56%	2.92%	-5.99%	-3.15%	-2.59%	2.60%	2.60%	-3.29%	0.98%	-1.69%	-0.68%	3.56%	Inf	Inf	0.67%	Inf	-5.68%	3.80%	-1.12%
		EiCentro	-2.09%	-1.87%	-1.18%	-0.88%	0.69%	0.69%	-1.87%	1.04%	2.78%	-1.80%	1.77%	-2.91%	Inf	Inf	1.01%	Inf	-1.57%	-2.38%	1.45%
TMCMC	-	Sin	5.63%	3.72%	-2.90%	-6.60%	-5.40%	-0.20%	1.99%	-7.00%	-0.70%	-3.94%	-5.43%	Inf	Inf	6.09%	Inf	2.67%	-9.00%	8.00%	
		EiCentro	-4.76%	-4.83%	-5.87%	-2.40%	-7.80%	-8.80%	5.16%	5.16%	9.00%	-6.07%	-9.49%	0.45%	Inf	Inf	-0.37%	Inf	-8.81%	-9.00%	-6.80%
	30	Sin	5.57%	-3.69%	-3.01%	6.79%	5.47%	2.03%	-0.53%	2.03%	6.45%	0.44%	-4.72%	-5.46%	Inf	Inf	-6.16%	Inf	-2.70%	-9.18%	-8.52%
		EiCentro	-4.77%	-4.88%	5.37%	2.83%	-6.99%	8.40%	5.22%	5.22%	-9.17%	-6.54%	-9.55%	0.75%	Inf	Inf	0.47%	Inf	-8.99%	9.16%	-7.01%
	10	Sin	5.05%	3.70%	-3.03%	-6.88%	5.51%	0.69%	0.69%	-1.98%	6.37%	-0.55%	-4.80%	-5.12%	Inf	Inf	6.23%	Inf	-2.76%	9.25%	-8.63%
		EiCentro	-4.79%	4.68%	-5.67%	-2.84%	-7.35%	8.83%	-5.63%	9.27%	9.27%	-7.04%	9.79%	-1.37%	Inf	Inf	2.09%	Inf	-7.38%	-8.42%	8.32%

IPV approach does not have error analysis of structural system parameter since the structural parameters are substituted by the architecture of neural network. Inf means the relative value of parameter identification accuracy cannot be computed in that there is a value assigned zero, but the absolute value of parameter identification accuracy can be calculated.

To make a restriction of the parameter space Θ , two side constraint vectors θ_{\min} and θ_{\max} are defined such that:

$$\theta_{\min}(i) \leq \theta(i) \leq \theta_{\max}(i) \quad 1 \leq i \leq d \quad (36)$$

The vector θ has specific constraints such that the generated initial samples can determine the feasible values that the parameters can take. By defining prior PDF of θ a uniform distribution between the likelihood PDF and side constraints are regarded as the prediction error assumed as Gaussian function distributed with unknown variance and zero mean. The prediction error is described as the error between the predicted system response and the simulated system response given by:

$$f(D|\theta) = \prod_{i=1}^l \frac{1}{\sigma_{acc}\sqrt{2\pi}} \exp\left[-\frac{1}{2\sigma_{acc}^2} \left(\frac{x(t_i) - \hat{x}(t_i|\theta)}{S_{acc}(t_i)}\right)^2\right] \quad (37)$$

where σ_{acc}^2 is the variance of the prediction errors and S_{acc} is the weighting function used to normalize the acceleration response of the hysteretic system. To achieve computational convenience, the log-likelihood function $\ln f(D|\theta)$ is employed in the actual implementation of the TMCMC algorithm as:

$$\ln f(D|\theta) = -\frac{1}{2}N_t \ln(2\pi) - N_t \ln(\sigma_{acc}) - \frac{1}{2\sigma_{acc}^2} \left(\frac{x(t_i) - \hat{x}(t_i|\theta)}{S_{acc}(t_i)}\right)^2 \quad (38)$$

The j^{th} stage of parameter evolution process by correspondingly choosing the values of p_j can be shown as the contours of PDF $f_j(\theta)$.

NUMERICAL ANALYSIS OF SYSTEM IDENTIFICATION

Parameter Settings

Table 1 lists the parameter assignments of the structural system associated with BWN hysteresis model for different cases. The mass coefficient of each floor is 1 kg, stiffness coefficient 10 N/m (sin) and 20 N/m (ElCentro), damping coefficient 0.05 N/(m/s) for each floor, respectively.

For hysteresis model, $A = 1, \alpha = 0.01, \beta = 2, \gamma = 2, n = 1$ (IPV), $n = 1.5$ (GA and TMCMC), $\delta_v = 0, \delta_{v1} = 1.5$ (sin) and 3 (ElCentro), $\delta_\eta = 0, \delta_{\eta1} = 1.5$ (sin) and 3 (ElCentro), $\sigma = 0.01, \delta_s = 0.05$. Damage occurrences are assumed at 30 s, 60 s, 100 s (sin) and 10 s, 20 s, 40 s (ElCentro) when both the strength degradation factor δ_v and stiffness degradation factor δ_η change to δ_{v1} and $\delta_{\eta1}$, respectively. For GA and TMCMC approaches, parameter initial values are assigned between the corresponding lower and upper bounds before the optimization processes. Parameters are updated between the two bounds of parametric searching space, and eventually achieve the exact values.

Numerical Analysis Results

Figures 7, 8 show the restoring force identification results when the structure is subjected to sinusoidal signal and

TABLE 3 | Correlation coefficient analysis for different cases.

Approach	SNR	Case	R-t3	R-t2	R-t1	R-x3	R-x2	R-x1	Running time(s)
IPV	-	Sin	1.0000	1.0000	1.0000	1.0000	1.0000	1.0000	85.11
		ElCentro	1.0000	1.0000	1.0000	1.0000	1.0000	1.0000	93.33
	30	Sin	0.9978	0.9991	0.9996	0.9978	0.9991	0.9996	89.93
		ElCentro	0.9969	0.9985	0.9991	0.9969	0.9985	0.9991	96.05
	10	Sin	0.8708	0.9273	0.9566	0.8708	0.9273	0.9566	95.67
		ElCentro	0.8243	0.8936	0.9314	0.8243	0.8936	0.9314	108.98
GA	-	Sin	0.9958	0.9964	0.9987	0.9958	0.9964	0.9997	901.31
		ElCentro	0.9667	0.9770	0.9869	0.9667	0.9770	0.9869	911.52
	30	Sin	0.9944	0.9952	0.9967	0.9944	0.9952	0.9967	908.25
		ElCentro	0.9662	0.9810	0.9859	0.9662	0.9810	0.9859	916.26
	10	Sin	0.8435	0.8924	0.9312	0.8435	0.8924	0.9312	927.76
		ElCentro	0.8012	0.8370	0.8994	0.8012	0.8370	0.8994	929.19
TMCMC	-	Sin	0.9983	0.9986	0.9988	0.9983	0.9986	0.9988	64812.36
		ElCentro	0.9925	0.9932	0.9957	0.9925	0.9932	0.9957	64901.47
	30	Sin	0.9108	0.9138	0.9259	0.9108	0.9138	0.9259	65012.69
		ElCentro	0.9018	0.9092	0.9129	0.9018	0.9092	0.9129	65109.53
	10	Sin	0.8360	0.8401	0.8498	0.8360	0.8401	0.8498	66409.77
		ElCentro	0.8209	0.8275	0.8302	0.8209	0.8275	0.8302	68014.28

The running time of system identification programs is computed using Samsung computer [Win 7 Ultimate, Processor: Intel (R), Xeon (R), CPU E3-1231 v3 @3.4G Hz, RAM: 8G, System type: 64 operating system].

ElCentro signal, respectively. Black curve represents the restoring force of the original structural system while the red curve represents the identified restoring force using IPV, GA, and TMCMC approaches. For the case of sinusoidal excitation, the identification results show that the degradation phenomenon of restoring forces of 2nd–3rd floor and 1st–2nd floor are more evident compared with ground-1st floor by using all of the three approaches. For the case of ElCentro excitation, the identification results show that the degradation phenomenon of restoring forces existing in all adjacent floors by using IPV and GA methods is more evident compared with that using TMCMC method. The hysteresis curves rotate accordingly when damage occurs. More results in details are discussed in the next section.

DISCUSSIONS

Choice of Signal Excitation Type and Objective Function

Both sinusoidal excitation signal and ElCentro excitation signal are used as input signals to the system identification of hysteric system. The frequency of sin signal is single and history curve is smooth and periodic variation. The ElCentro wave is stochastic, non-periodic, and non-steady state, and this represents the other type of excitation which is totally counter to harmonic wave such as sin signal. These two types of signals are employed to the response analysis and verification of the generalization capability of three different algorithms for identifying restoring forces of hysteretic structure. In addition, the establishment of objective functions employed in the GA and TMCMC are formulated through the combination of desired and simulated acceleration signal differences of all three degrees of freedom.

Parameter Choice for System Identification

Table 2 shows the parameter identification error using GA and TMCMC for the case of noise free, SNR = 30 and SNR = 10 (SNR = signal noise ratio). These error represents the relative error between the “true value” and “identified value.” All errors are no more than 10%. Generally for the cases with higher SNR they perform better parameter identification results since the disturbance of noise to signal is low. From Figures 7, 8, and Table 2, for the noise free case, it is shown that during the degradation process (damage evolution), strength degradation factor δ_v changes from 0 to 1.4695 (sin,GA) /3.0130 (ElCentro,GA) /1.5913 (sin,TMCMC) /2.9890 (ElCentro,TMCMC), and stiffness degradation factor δ_η changes from 0 to 1.5370 (sin,GA)/2.9142 (ElCentro,GA)/1.5400 (sin,TMCMC)/2.7357 (ElCentro,TMCMC).

The hysteresis loop rotates clockwise with a certain degree, indicating large non-linearity and considerable degradation. However, from the identification results, it is also found that in the sin excitation case, the hysteresis loop exhibits better slip-lock phenomenon, and can absorb more energy than the case of ElCentro excitation. Noise corrupted cases have similar parameter identification results.

Table 3 shows the analysis of correlation coefficients for different cases. For the cases with small SNR, the identification effectiveness is not relatively good compared with noise free and

TABLE 4 | Degradation parameter assignment for different cases.

Approach	Case	Parameter	Group 1			Group 2			Group 3			Group 4			Group 5													
			δ_v	δ_{v1}	δ_η	$\delta_{\eta1}$	δ_v	δ_{v1}	δ_η	$\delta_{\eta1}$	δ_v	δ_{v1}	δ_η	$\delta_{\eta1}$	δ_v	δ_{v1}	δ_η	$\delta_{\eta1}$										
IPV	Sin	-	0	1.5	0	1.8	0	1.8	0	2.1	0	2.1	0	2.4	0	2.4	0	2.7	0	2.7	0	4.2	0	4.2				
	ElCentro	-	0	3	0	3.3	0	3.3	0	3.6	0	3.6	0	3.9	0	3.9	0	4.2	0	4.2	0	4.2	0	4.2				
GA	Sin	True value	0	1.5	0	1.5	0	1.5	0	1.5	0	1.5	0	1.5	0	1.8	0	1.8	0	2.1	0	2.1	0	2.1	0	2.1		
		Lower bound	0	0.1	0	0.1	0	0.5	0	0.5	0	1	0	1	0	1	0	1	0	1	0	1	0	1	0	1	0	1
	ElCentro	Upper bound	0.1	3	0.1	3	0.1	2.5	0.1	2.5	0.1	2	0.1	2	0.1	3.6	0.1	3.6	0.1	4.2	0.1	4.2	0.1	4.2	0.1	4.2		
		True value	0	3	0	3	0	3	0	3	0	3	0	3	0	3.3	0	3.3	0	3.6	0	3.6	0	3.6	0	3.6		
TMCMC	Sin	Lower bound	0	0.1	0	0.1	0	1	0	1	0	2	0	2	0	0.1	0	0.1	0	0.1	0	0.1	0	0.1	0	0.1	0	0.1
		Upper bound	0.1	6	0.1	6	0.1	5	0.1	5	0.1	4	0.1	4	0.1	6.6	0.1	6.6	0.1	7.2	0.1	7.2	0.1	7.2	0.1	7.2		
TMCMC	Sin	True value	0	1.5	0	1.5	0	1.5	0	1.5	0	1.5	0	1.5	0	1.8	0	1.8	0	2.1	0	2.1	0	2.1	0	2.1		
		Lower bound	0	0.1	0	0.1	0	0.5	0	0.5	0	1	0	1	0	1	0	1	0	1	0	1	0	1	0	1		
	ElCentro	Upper bound	0.1	3	0.1	3	0.1	2.5	0.1	2.5	0.1	2	0.1	2	0.1	3.6	0.1	3.6	0.1	4.2	0.1	4.2	0.1	4.2	0.1	4.2		
		True value	0	3	0	3	0	3	0	3	0	3	0	3	0	3.3	0	3.3	0	3.6	0	3.6	0	3.6	0	3.6		
TMCMC	ElCentro	Lower bound	0	0.1	0	0.1	0	1	0	1	0	2	0	2	0	0.1	0	0.1	0	0.1	0	0.1	0	0.1	0	0.1		
		Upper bound	0.1	6	0.1	6	0.1	5	0.1	5	0.1	4	0.1	4	0.1	6.6	0.1	6.6	0.1	7.2	0.1	7.2	0.1	7.2	0.1	7.2		

Data in the gray area represents that for the same case, it has the same “true value” but different lower and upper bounds.

higher SNR (R-t is the restoring force-time relationship, and R-x is the restoring force-relative displacement relationship).

In this paper, IPV is a radius basis neural network which is a completely data-driven approach, while GA and TMCMC are not fully data-driven in that they assign the identification model within specific initial parameter intervals and then update and search to optimize structural model.

IPV method performs better identification results due to its adaptive learning capability and anti noise property in the noise environment. From computational time, it can be concluded that the IPV approach is a more efficient identification method compared with GA and TMCMC methods. Concretely, for the case of noise free, the computational time for GA and TMCMC are 9.59 and 760.51% longer than IPV (sin), and 8.77 and 694.40% longer than IPV (ElCentro). Similar results are also shown in noise corrupted cases. This demonstrates IPV method has higher computational efficiency than GA and TMCMC approaches.

Strength and stiffness degradation parameters are both very important in the hysteresis model, which determine the

hysteretic behavior of structural systems. **Table 4** lists five groups of parameter assignments regarding the variance of strength and stiffness degradation coefficients. The objective of setting these cases is studying the influence of change of degradation parameters on system identification accuracy.

To simulate damage occurrence, for IPV approach, strength degradation factor δ_v and stiffness degradation factor δ_η change from 1.5 to 1.8, 2.1, 2.4, and 2.7, respectively (sin), while change from 3 to 3.3, 3.6, 3.9, and 4.2, respectively (ElCentro). For GA (sin) method, for the first three groups, the true value of strength degradation factor δ_v and stiffness degradation factor δ_η keep fixed value 1.5 but the lower and upper bound change from 0.1–3 to 0.5–2.5 and 1–2, respectively. For the last two groups, the true value of strength degradation factor δ_v and stiffness degradation factor δ_η are 1.8 and 2.1, respectively but the lower and upper bound correspondingly change from 0.1 to 3.6 and 0.1 to 4.2, respectively.

For GA (ElCentro) method, for the first three groups, the true value of strength degradation factor δ_v and stiffness degradation factor δ_η keep fixed value 3 but the lower and upper bound

TABLE 5 | Correlation coefficient analysis (IPV).

Approach	Group	SNR	Case	R-t3	R-t2	R-t1	R-x3	R-x2	R-x1	Running time(s)	
IPV	1	–	Sin	1.0000	1.0000	1.0000	1.0000	1.0000	1.0000	85.11	
			ElCentro	1.0000	1.0000	1.0000	1.0000	1.0000	1.0000	93.33	
	30	Sin	Sin	0.9978	0.9991	0.9996	0.9978	0.9991	0.9996	89.93	
			ElCentro	0.9969	0.9985	0.9991	0.9969	0.9985	0.9991	96.05	
		10	Sin	0.8708	0.9273	0.9566	0.8708	0.9273	0.9566	95.67	
			ElCentro	0.8243	0.8936	0.9314	0.8243	0.8936	0.9314	108.98	
	2	–	Sin	1.0000	0.9999	1.0000	1.0000	0.9999	1.0000	89.01	
			ElCentro	1.0000	1.0000	1.0000	1.0000	1.0000	1.0000	92.17	
		30	Sin	0.9975	0.9984	0.9993	0.9975	0.9984	0.9993	95.11	
			ElCentro	0.9957	0.9960	0.9971	0.9957	0.9960	0.9971	98.02	
			10	Sin	0.8567	0.8580	0.8700	0.8567	0.8580	0.8700	104.78
				ElCentro	0.8108	0.8179	0.8244	0.8108	0.8179	0.8244	115.90
	3	–	Sin	0.9999	1.0000	1.0000	0.9999	1.0000	1.0000	88.97	
			ElCentro	0.9999	1.0000	1.0000	0.9999	1.0000	1.0000	90.00	
		30	Sin	0.9967	0.9976	0.9987	0.9967	0.9976	0.9987	96.02	
			ElCentro	0.9955	0.9965	0.9973	0.9955	0.9965	0.9973	99.14	
			10	Sin	0.8607	0.8678	0.8711	0.8607	0.8678	0.8711	107.37
				ElCentro	0.8236	0.8299	0.8317	0.8236	0.8299	0.8317	120.03
	4	–	Sin	1.0000	1.0000	0.9999	1.0000	1.0000	0.9999	83.12	
			ElCentro	1.0000	1.0000	0.9999	1.0000	1.0000	0.9999	87.21	
		30	Sin	0.9970	0.9976	0.9984	0.9970	0.9976	0.9984	95.09	
			ElCentro	0.9961	0.9973	0.9979	0.9961	0.9973	0.9979	97.33	
			10	Sin	0.8700	0.8736	0.8744	0.8700	0.8736	0.8744	100.20
				ElCentro	0.8301	0.8315	0.8333	0.8301	0.8315	0.8333	107.69
5	–	Sin	1.0000	0.9999	0.9999	1.0000	0.9999	0.9999	86.09		
		ElCentro	0.9999	0.9999	0.9999	0.9999	0.9999	0.9999	89.11		
	30	Sin	0.9968	0.9977	0.9990	0.9968	0.9977	0.9990	93.84		
		ElCentro	0.9957	0.9969	0.9980	0.9957	0.9969	0.9980	98.94		
		10	Sin	0.8657	0.8672	0.8680	0.8657	0.8672	0.8680	104.55	
			ElCentro	0.8489	0.8498	0.8524	0.8489	0.8498	0.8524	111.11	

change from 0.1–6 to 1–5 and 2–4, respectively. For the last two groups, the true value of strength degradation factor δ_v and stiffness degradation factor δ_n are 3.3 and 3.6, respectively but the lower and upper bound correspondingly change from 0.1 to 6.6 and 0.1 to 7.2, respectively. TMCMC parameter assignment has similar cases.

Table 5 shows the influence of change of strength and stiffness degradation parameter on system identification accuracy indicated by correlation coefficients using IPV method. For sin excitation, as the strength and stiffness degradation parameter increase from 1.5 to 2.7, the correlation coefficients do not increase or decrease for the same case, and the computational time also keep almost unchanged: (sin) Group1: 85.11–95.67 s, Group 2: 89.01–104.78 s, Group 3: 88.97–107.37 s, Group 4: 83.12–100.20 s, Group 5: 86.09–104.55 s. (ElCentro) Group 1: 93.33–108.98 s, Group 2: 92.17–115.90 s, Group 3: 90.00–120.03 s, Group 4: 87.21–107.69 s, Group 5: 89.11–111.11 s.

Table 6 shows the influence of change of strength and stiffness degradation parameter on system identification accuracy indicated by correlation coefficients using GA method. For sin

excitation, when the strength and stiffness degradation parameter value is fixed at 1.5, as bounds (interval) change from 0–3 to 1–2, the correlation coefficients approach 1, indicating the system identification accuracy improves with the bound interval decreasing. The closer the bounds approach to the true value, the more accurate and deterministic the system identification results are. Accordingly, the computational time decreases with the bound interval decreasing. For details: Group 1: 901.31–927.76 s, Group 2: 895.66–922.22 s, Group 3: 889.73–914.73 s. When the true value of strength and stiffness degradation increases from 1.5 to 2.1 with given bounds, the identification accuracy decreases, and the computational time increases accordingly. Similar cases can also be found for ElCentro excitation signal.

Table 7 shows the influence of change of strength and stiffness degradation parameter on system identification accuracy indicated by correlation coefficients using TMCMC method. For sin excitation, when the strength and stiffness degradation parameter value is fixed at 1.5, as bounds (interval) change from 0–3 to 1–2, the correlation coefficients approach 1, indicating the

TABLE 6 | Correlation coefficient analysis (GA).

Approach	Group	SNR	Case	R-t3	R-t2	R-t1	R-x3	R-x2	R-x1	Running time(s)
GA	1	–	Sin	0.9958	0.9964	0.9987	0.9958	0.9964	0.9997	901.31
			ElCentro	0.9667	0.9770	0.9869	0.9667	0.9770	0.9869	911.52
	30	–	Sin	0.9944	0.9952	0.9967	0.9944	0.9952	0.9967	908.25
			ElCentro	0.9662	0.9810	0.9859	0.9662	0.9810	0.9859	916.26
	10	–	Sin	0.8435	0.8924	0.9312	0.8435	0.8924	0.9312	927.76
			ElCentro	0.8012	0.8370	0.8994	0.8012	0.8370	0.8994	929.19
	2	–	Sin	0.9963	0.9968	0.9993	0.9963	0.9968	0.9993	895.66
			ElCentro	0.9700	0.9797	0.9888	0.9700	0.9797	0.9888	903.65
	30	–	Sin	0.9947	0.9958	0.9971	0.9947	0.9958	0.9971	906.59
			ElCentro	0.9668	0.9831	0.9877	0.9668	0.9831	0.9877	912.28
	10	–	Sin	0.8553	0.9012	0.9337	0.8553	0.9012	0.9337	922.22
			ElCentro	0.8108	0.8433	0.9042	0.8108	0.8433	0.9042	925.59
	3	–	Sin	0.9970	0.9976	0.9995	0.9970	0.9976	0.9995	889.73
			ElCentro	0.9712	0.9800	0.9923	0.9712	0.9800	0.9923	894.49
	30	–	Sin	0.9952	0.9967	0.9979	0.9952	0.9967	0.9979	900.01
			ElCentro	0.9711	0.9828	0.9880	0.9711	0.9828	0.9880	905.38
	10	–	Sin	0.8573	0.9103	0.9355	0.8573	0.9103	0.9355	914.73
			ElCentro	0.8098	0.8449	0.9098	0.8098	0.8449	0.9098	918.90
	4	–	Sin	0.9813	0.9877	0.9921	0.9813	0.9877	0.9921	917.74
			ElCentro	0.9512	0.9657	0.9703	0.9512	0.9657	0.9703	926.54
	30	–	Sin	0.9754	0.9779	0.9837	0.9754	0.9779	0.9837	930.07
			ElCentro	0.9534	0.9600	0.9718	0.9534	0.9600	0.9718	942.83
	10	–	Sin	0.8301	0.8544	0.9009	0.8301	0.8544	0.9009	951.11
			ElCentro	0.7885	0.8177	0.8836	0.7885	0.8177	0.8836	958.98
5	–	Sin	0.9689	0.9788	0.9864	0.9689	0.9788	0.9864	926.34	
		ElCentro	0.9321	0.9555	0.9688	0.9321	0.9555	0.9688	929.88	
30	–	Sin	0.9500	0.9633	0.9773	0.9500	0.9633	0.9773	937.48	
		ElCentro	0.9412	0.9678	0.9006	0.9412	0.9678	0.9006	940.05	
10	–	Sin	0.9378	0.9538	0.9699	0.9378	0.9538	0.9699	956.01	
		ElCentro	0.7650	0.7948	0.8305	0.7650	0.7948	0.8305	968.44	

TABLE 7 | Correlation coefficient analysis (TMCMC).

Approach	Group	SNR	Case	R-t3	R-t2	R-t1	R-x3	R-x2	R-x1	Running time(s)
TMCMC	1	-	Sin	0.9983	0.9986	0.9988	0.9983	0.9986	0.9988	64812.36
			ElCentro	0.9925	0.9932	0.9957	0.9925	0.9932	0.9957	64901.47
		30	Sin	0.9108	0.9138	0.9259	0.9108	0.9138	0.9259	65012.69
			ElCentro	0.9018	0.9092	0.9129	0.9018	0.9092	0.9129	65109.53
		10	Sin	0.8360	0.8401	0.8498	0.8360	0.8401	0.8498	66409.77
			ElCentro	0.8209	0.8275	0.8302	0.8209	0.8275	0.8302	68014.28
	2	-	Sin	0.9985	0.9989	0.9990	0.9985	0.9989	0.9990	63508.90
			ElCentro	0.9930	0.9941	0.9964	0.9930	0.9941	0.9964	63132.56
		30	Sin	0.9112	0.9143	0.9265	0.9112	0.9143	0.9265	64657.77
			ElCentro	0.9034	0.9106	0.9244	0.9034	0.9106	0.9244	64789.88
		10	Sin	0.8373	0.8456	0.8543	0.8373	0.8456	0.8543	65546.11
			ElCentro	0.8215	0.8288	0.8376	0.8215	0.8288	0.8376	66444.90
	3	-	Sin	0.9988	0.9990	0.9993	0.9988	0.9990	0.9993	62109.67
			ElCentro	0.9935	0.9957	0.9970	0.9935	0.9957	0.9970	62476.67
		30	Sin	0.9118	0.9156	0.9279	0.9118	0.9156	0.9279	63157.58
			ElCentro	0.9056	0.9117	0.9279	0.9056	0.9117	0.9279	63654.59
		10	Sin	0.8384	0.8491	0.8579	0.8384	0.8491	0.8579	64111.67
			ElCentro	0.8244	0.8296	0.8383	0.8244	0.8296	0.8383	65000.78
	4	-	Sin	0.9867	0.9889	0.9902	0.9867	0.9889	0.9902	65457.89
			ElCentro	0.9756	0.9780	0.9806	0.9756	0.9780	0.9806	65989.07
		30	Sin	0.9000	0.9067	0.9138	0.9000	0.9067	0.9138	66675.88
			ElCentro	0.8923	0.8979	0.9036	0.8923	0.8979	0.9036	66899.04
		10	Sin	0.8222	0.8318	0.8440	0.8222	0.8318	0.8440	67476.68
			ElCentro	0.8016	0.8066	0.8148	0.8016	0.8066	0.8148	68698.36
	5	-	Sin	0.9659	0.9770	0.9799	0.9659	0.9770	0.9799	66780.77
			ElCentro	0.9502	0.9589	0.9664	0.9502	0.9589	0.9664	66999.75
		30	Sin	0.8879	0.8909	0.9008	0.8879	0.8909	0.9008	67376.11
			ElCentro	0.8748	0.8765	0.8800	0.8748	0.8765	0.8800	67980.04
		10	Sin	0.8117	0.8277	0.8335	0.8117	0.8277	0.8335	68780.99
			ElCentro	0.7980	0.8034	0.8110	0.7980	0.8034	0.8110	69333.56

system identification accuracy improves with the bound interval decreasing.

The closer the bounds approach to the true value, the more accurate and deterministic the system identification results are. Accordingly, the computational time decreases with the bound interval value decreasing, as shown in detailed cases: Group 1: 64812.36–66409.77 s, Group 2: 63508.90–65546.11 s, Group 3: 62109.67–64111.67 s. When the true value of strength and stiffness degradation increases from 1.5 to 2.1 with given bounds, the identification accuracy decreases, and the computational time increases accordingly. Similar cases can also be found for ElCentro excitation signal.

Comparison of Three Different Algorithm Principles

Intelligent Parameter Varying approach uses radial basis function to map the complex input signal to high dimensional signal, and it is a data driven mechanism. By using appropriate error back propagation mechanism, this method can design a good neural network architecture to process considerable amount of data or high parameter dimension, especially for system

identification application. Genetic algorithm and Transitional Markov Chain Monte Carlo approaches are non-data-driven intelligent optimization algorithms. Genetic algorithm optimizes the parameters by using selection, crossover, and mutation operators through elitist strategy. Transitional Markov Chain Monte Carlo method employs model updating to optimize parameters through applying Bayesian inference with TMCMC probabilistic simulations, and the samples eventually populate well in the high probability region of the posterior PDFs close to the true model parameters through a series of intermediate updating processes. The latter two methods are related to optimization theory, and may not perform well (tapped in local optimum) especially when the parameter dimension is relatively large. Therefore, it is very significant to conduct a comparative study on system identification of hysteretic structures using Intelligent Parameter Varying, Genetic Algorithm and Transitional Markov Chain Monte Carlo methods.

The above discussions regarding the choice of signal excitation type, parameter choice for system identification and comparison between three different principles for system identification has

demonstrated the necessity, feasibility and importance of this research. It also illustrates the generalization of this research and proves the superiority using IPV over GA and TMCMC for system identification of hysteretic structures.

CONCLUSIONS

To better understand the hysterically degrading, structural systems using an earlier version of smoothly varying Bouc-Wen-Baber-Noori hysteresis model in this research, a detailed description of BWBN hysteresis model is presented, and the restoring force and the associated system variables are analyzed using non-linear differential equations containing different parameters. By choosing the parameters in a suitable way, it is possible to generate a large variety of different shapes of the hysteresis loops. A three floor shear structure is modeled which composes of three adjacent subsystems by associating system kinetic equations, restoring force expression and BWBN hysteresis model. By using BWB-Noori model, a new scheme is proposed to effectively and efficiently track and estimate the hysteretic restoring forces using intelligent parameter varying approach, genetic optimization algorithm and the transitional Markov Chain Monte Carlo simulation. Most importantly, comparative study by using these approaches for different cases is demonstrated through parameter error analysis and correlation coefficient analysis of system identification of time varying degrading structures. Major findings are summarized in the following statements.

- (1) BWBN hysteresis model is a smoothly varying differential mathematical model, and it can reflect highly non-linear and gradual hysteretic degradation with slip lock behavior observed in numerous structural and mechanical systems, and this model can be widely used to predict the response of degradation phenomena of general structures.
- (2) When employing system identification and parameter/model updating approach, the initial parameter spaces of the hysteretic system should be well assigned to satisfy the requirement of reliable system identification process. Tracking of the restoring forces for the hysteretic system using system identification approaches can accurately estimate the changing of restoring force status in time, i.e., the rotation of hysteresis loops indicates structural degradation due to abrupt damages. This proves that system

identification techniques can be used as powerful tools for detecting the damage/degradation for structural health monitoring applications. Stiffness and damping terms are lumped into restoring forces represented by structural non-linearity, and this constructs effective IPV modeling.

- (3) IPV, GA, and TMCMC methods are employed for the system identification of BWBN model, and a comparative study is conducted for the verification of the effectiveness of these approaches. The results show higher SNR cases have better correlation and smaller parameter errors. From the correlation analysis, we also know that IPV has better anti-noise capability than GA and TMCMC.
- (4) Qualitative comparison regarding the computational time of these three different algorithms are ranked for different cases, i.e., IPV Based system identification approach < GA based system identification method << TMCMC based system identification approach. This demonstrates that compared with traditional parameter optimization and statistical methods, IPV approach is a promising, efficient and effective way for system identification and Structural Health Monitoring applications.
- (5) IPV technique using the RBF based ANNs has its superior advantages over the GA based identification and the TMCMC based identification techniques for its fully data-driven adaptive learning ability for high dimensional data. Proper design of parameter initial bounds can improve the computational efficiency for GA and TMCMC approaches. The GA based identification may have relatively uncertain values for the randomness of genetic operations (selection, crossover, and mutation), while the TMCMC algorithm is based on the sampling technique that is not as effective and is uncertain, especially for the case that the system has a relatively large number of parameters.

AUTHOR CONTRIBUTIONS

YZ as Ph.D. student. MN as main supervisor. WA supervisor. TA was invited, due to his expertise in the area of Genetic Algorithms, to join the paper as a co-author. TA carefully reviewed the technical analysis and independently carried out a system ID using Genetic Algorithm. His contributions were valuable in this regard and thus, his name is added in the newly revised version.

REFERENCES

- Abouelwafa, M. N., El-Gamal, H. A., Mohamed, Y. S., and Altabay, W. A. (2014). An expert system for life prediction of woven-roving GFRE closed end thick tube subjected to combined bending moments and internal hydrostatic pressure using artificial neural network. *Int. J. Adv. Mater. Res.* 845, 12–17. doi: 10.4028/www.scientific.net/AMR.845.12
- Altabay, W. A. (2014). "Vibration analysis of laminated composite variable thickness plate using finite strip transition matrix technique and MATLAB verifications," in *MATLAB- Particular for Engineer*, ed K. Bennett (InTech), 583–620.
- Altabay, W. A. (2016). FE and ANN model of ECS to simulate the pipelines suffer from internal corrosion. *Struct. Monit. Mainten.* 3, 297–314. doi: 10.12989/smm.2016.3.3.297
- Altabay, W. A. (2017a). An exact solution for mechanical behavior of BFRP Nano-thin films embedded in NEMS. *J. Adv. Nano Res.* 5, 337–357. doi: 10.12989/anr.2017.5.4.337
- Altabay, W. A. (2017b). Free vibration of basalt fiber reinforced polymer (FRP) laminated variable thickness plates with intermediate elastic support using finite strip transition matrix (FSTM) method. *J. Vibroeng.* 19, 2873–2885. doi: 10.21595/jve.2017.18154
- Altabay, W. A. (2017c). Prediction of natural frequency of basalt fiber reinforced polymer (FRP) laminated variable thickness plates with intermediate elastic

- support using artificial neural networks (ANNs) method. *J. Vibroeng.* 19, 3668–3678. doi: 10.21595/jve.2017.18209
- Altabay, W. A. (2017d). Delamination evaluation on basalt FRP composite pipe by electrical potential change. *J. Adv. Aircraft Spacecraft Sci.* 4, 515–528. doi: 10.12989/aas.2017.4.5.515
- Altabay, W. A. (2017e). EPC method for delamination assessment of basalt FRP pipe: electrodes number effect. *J. Struct. Monit. Mainten.* 4, 69–84. doi: 10.12989/smm.2017.4.1.069
- Altabay, W. A. (2018). High performance estimations of natural frequency of basalt FRP laminated plates with intermediate elastic support using response surfaces method. *J. Vibroeng.* 20, 1099–1107. doi: 10.21595/jve.2017.18456
- Altabay, W. A., and Noori, M. (2017a). Detection of fatigue crack in basalt FRP laminate composite pipe using electrical potential change method. *J. Phys. Conf. Ser.* 842:012079. doi: 10.1088/1742-6596/842/1/012079
- Altabay, W. A., and Noori, M. (2017b). Fatigue life prediction for carbon fibre/epoxy laminate composites under spectrum loading using two different neural network architectures. *Int. J. Sustain. Mater. Struct. Syst.* 3, 53–78. doi: 10.1504/IJSMSS.2017.092252
- Altabay, W. A., and Noori, M. (2018). Monitoring the water absorption in GFRE pipes via an electrical capacitance sensors. *J. Adv. Aircraft Spacecraft Sci.* 5, 411–434. doi: 10.12989/aas.2018.5.4.499
- Baber, T. T., and Noori, M. N. (1985). Random vibration of degrading, pinching systems. *J. Eng. Mech.* 111, 1010–1026. doi: 10.1061/(ASCE)0733-9399(1985)111:8(1010)
- Baber, T. T., and Noori, M. N. (1986). Modeling general hysteresis behavior and random vibration application. *J. Vib. Acoust.* 108, 411–420. doi: 10.1115/1.3269364
- Baber, T. T., and Wen, Y. K. (1980). *Stochastic Equivalent Linearization for Hysteretic, Degrading, Multistory Structures*. University of Illinois Engineering Experiment Station; College of Engineering; University of Illinois at Urbana-Champaign.
- Beck, J. L., and Au, S. K. (2002). Bayesian updating of structural models and reliability using Markov chain Monte Carlo simulation. *J. Eng. Mech.* 128, 380–391. doi: 10.1061/(ASCE)0733-9399(2002)128:4(380)
- Behmanesh, I., and Moaveni, B. (2014). Probabilistic identification of simulated damage on the Dowling Hall footbridge through Bayesian finite element model updating. *J. Struct. Control Health Monit.* 22, 463–483. doi: 10.1002/stc.1684
- Bouc, R. (1967). “Forced vibration of mechanical systems with hysteresis,” in *Proceedings of the Fourth Conference on Non-linear Oscillation* (Prague).
- Brewick, P. T., Masri, S. F., Carboni, B., and Lacarbonara, W. (2016). Data-based nonlinear identification and constitutive modeling of hysteresis in NiTiNOL and steel strands. *J. Eng. Mech.* 142, 1–17. doi: 10.1061/(ASCE)EM.1943-7889.0001170
- Chan, R., Yuen, J., Lee, E., and Arashpour, M. (2015). Application of nonlinear-autoregressive-exogenous model to predict the hysteretic behaviour of passive control systems. *J. Eng. Struct.* 85, 1–10. doi: 10.1016/j.engstruct.2014.12.007
- Charalampakis, A. E., and Dimou, C. K. (2010). Identification of Bouc–Wen hysteretic systems using particle swarm optimization. *J. Comput. Struct.* 88, 1197–1205. doi: 10.1016/j.compstruc.2010.06.009
- Charalampakis, A. E., and Koumousis, V. K. (2008a). Identification of Bouc–Wen hysteretic systems by a hybrid evolutionary algorithm. *J. Sound Vib.* 314, 571–585. doi: 10.1016/j.jsv.2008.01.018
- Charalampakis, A. E., and Koumousis, V. K. (2008b). On the response and dissipated energy of Bouc–Wen hysteretic model. *J. Sound Vib.* 309, 887–895. doi: 10.1016/j.jsv.2007.07.080
- Chatzi, E. N., and Smyth, A. W. (2009). The unscented Kalman filter and particle filter methods for nonlinear structural system identification with non-collocated heterogeneous sensing. *J. Struct. Control Health Monit.* 16, 99–123. doi: 10.1002/stc.290
- Chatzi, E. N., Smyth, A. W., and Masri, S. F. (2010). Experimental application of on-line parametric identification for nonlinear hysteretic systems with model uncertainty. *J. Struct. Saf.* 32, 326–337. doi: 10.1016/j.strusafe.2010.03.008
- Ching, J., and Chen, Y. C. (2007). Transitional Markov Chain Monte Carlo method for Bayesian model updating, model class selection, and model averaging. *J. Eng. Mech.* 133, 816–832. doi: 10.1061/(ASCE)0733-9399(2007)133:7(816)
- Constantinou, M. C., Soong, T. T., and Dargush, G. F. (1998). *Passive Energy Dissipation Systems for Structural Design and Retrofit*. Multidisciplinary Center for Earthquake Engineering Research.
- Deb, K. (2013). *Bouc-Wen-Baber-Noori Model of Hysteresis*. Source Forge. Available online at: <https://sourceforge.net/projects/boucwenbabernoo/>
- Deb, K., Pratap, A., Agarwal, S., and Meyarivan, T. (2002). A fast and elitist multi-objective genetic algorithm: NSGA-II. *IEEE J. Trans. Evol. Comput.* 6, 182–197. doi: 10.1109/4235.996017
- Erazo, K., and Nagarajaiah, S. (2018). Bayesian structural identification of a hysteretic negative stiffness earthquake protection system using unscented Kalman filtering. *J. Struct. Control Health Monit.* 25, 1–18. doi: 10.1002/stc.2203
- Foliente, G. C. (1995). Hysteresis modeling of wood joints and structural systems. *J. Struct. Eng.* 121, 1013–1022. doi: 10.1061/(ASCE)0733-9445(1995)121:6(1013)
- Green, P. L. (2015). Bayesian system identification of dynamical systems using large sets of training data: a MCMC solution. *J. Probabilist. Eng. Mech.* 42, 54–63. doi: 10.1016/j.probenmech.2015.09.010
- Green, P. L., Cross, E. J., and Worden, K. (2015). Bayesian system identification of dynamical systems using highly informative training data. *J. Mech. Syst. Signal PR* 56, 109–122. doi: 10.1016/j.ymsp.2014.10.003
- Hornig, K. H., and Flowers, G. T. (2005). Parameter characterization of the Bouc–Wen mechanical hysteresis model for sandwich composite materials using real coded genetic algorithms. *Int. J. Acoust. Vib.* 10:7381. doi: 10.20855/ijav.2005.10.2176
- Hossain, M. R. (1995). *OpenSees Structural Design Software Command Manual for BWN Material Model*. Available online at: http://opensees.berkeley.edu/wiki/index.php/BWBN_Material
- Ikhouane, F., and Gomis-Bellmunt, O. (2008). A limit cycle approach for the parametric identification of hysteretic systems. *J. Syst. Control Lett.* 57, 663–669. doi: 10.1016/j.sysconle.2008.01.003
- Ikhouane, F., Mañosa, V., and Rodellar, J. (2007). Dynamic properties of the hysteretic Bouc–Wen model. *J. Syst. Control Lett.* 56, 197–205. doi: 10.1016/j.sysconle.2006.09.001
- Ikhouane, F., and Rodellar, J. (2007). *Systems With Hysteresis: Analysis, Identification and Control Using the Bouc–Wen Model*. Hong Kong: John Wiley & Sons.
- Jeon-Shang, L., and Yigong, Z. (1994). Nonlinear structural identification using extended Kalman filter. *J. Comput. Struct.* 52, 757–764.
- Kontoroupi, T., and Smyth, A. W. (2017). Online Bayesian model assessment using nonlinear filters. *J. Struct. Control Health Monit.* 24, 1–15. doi: 10.1002/stc.1880
- Lei, Y., and Jiang, Y. Q. (2011). “A two-stage Kalman estimation approach for the identification of structural parameters under unknown inputs,” in *The Twelfth East Asia-Pacific Conference on Structural Engineering and Construction*, 3088–3094.
- Ljung, L. (2010). Perspectives on system identification. *Annu. Rev. Control* 34, 1–5. doi: 10.1016/j.arcontrol.2009.12.001
- Lu, S., and Basar, T. (1998). Robust nonlinear system identification using neural-network models. *IEEE T. Neural Netw.* 9, 407–429. doi: 10.1109/72.668883
- Ma, F., Zhang, H., Bockstedte, A., Foliente, G. C., and Paevere, P. (2004). Parameter analysis of the differential model of hysteresis. *J. Appl. Mech.* 71, 342–349. doi: 10.1115/1.1668082
- Masri, S. F., Chassiakos, A. G., and Caughey, T. K. (1992). Structure-unknown non-linear dynamic systems: identification through neural networks. *J. Smart Mater. Struct.* 1, 45–56. doi: 10.1088/0964-1726/1/1/007
- Monti, G., Quaranta, G., and Marano, G. C. (2009). Genetic-algorithm-based strategies for dynamic identification of nonlinear systems with noise-corrupted response. *J. Comput. Civil Eng.* 24, 173–187. doi: 10.1061/(ASCE)CP.1943-5487.0000024
- Mu, T., Zhou, L., and Yang, J. N. (2013). Comparison of adaptive structural damage identification techniques in nonlinear hysteretic vibration isolation systems. *J. Earthq. Eng. Eng. Vib.* 12, 659–667. doi: 10.1007/s11803-013-0204-y
- Muller, O., Savino, F., Rubinstein, M., and Foschi, R. O. (2012). “Performance-based seismic design: a search-based cost optimization with minimum reliability constraints,” in *Structural Seismic Design Optimization and Earthquake Engineering: Formulations and Applications* 23–50. doi: 10.4018/978-1-4666-1640-0.ch002
- Muto, M., and Beck, J. L. (2008). Bayesian updating and model class selection for hysteretic structural models using stochastic simulation. *J. Vib. Control* 14, 7–34. doi: 10.1177/1077546307079400
- Muto, M. M. (2007). *Application of Stochastic Simulation Methods to System Identification*. Ph.D., California Institute of Technology.

- Narendra, K. S., and Parthasarathy, K. (1990). Identification and control of dynamical systems using neural networks. *IEEE T. Neural Netw.* 1, 4–27. doi: 10.1109/72.80202
- Noori, M. (1984). *Random Vibration of Degrading Systems With General Hysteretic Behavior*. Ph.D., University of Virginia.
- Noori, M., Wang, H., Altabay, W. A., and Silik, A. I. H. (2018). A modified wavelet energy rate based damage identification method for steel bridges. *Int. J. Sci. Technol.* doi: 10.24200/sci.2018.20736
- Ortiz, G. A., Alvarez, D. A., and Bedoya-Ruiz, D. (2013). Identification of Bouc-Wen type models using multi-objective optimization algorithms. *J. Comput. Struct.* 114, 121–132. doi: 10.1016/j.compstruc.2012.10.016
- Ortiz, G. A., Alvarez, D. A., and Bedoya-Ruiz, D. (2015). Identification of Bouc-Wen type models using the Transitional Markov Chain Monte Carlo method. *J. Comput. Struct.* 146, 252–269. doi: 10.1016/j.compstruc.2014.10.012
- Park, Y. J., Wen, Y. K., and Ang, A. (1986). Random vibration of hysteretic systems under bi-directional ground motions. *Earthq. Eng. Struct. D* 14, 543–557. doi: 10.1002/eqe.4290140405
- Peng, G. R., Li, W. H., Du, H., Deng, H. X., and Alicia, G. (2014). Modelling and identifying the parameters of a magneto-rheological damper with a force-lag phenomenon. *J. Appl. Math. Model.* 38, 3763–3773. doi: 10.1016/j.apm.2013.12.006
- Puttige, V. R., and Anavatti, S. G. (2007). “Comparison of real-time online and offline neural network models for a UAV,” in *IEEE International Joint Conference on Neural Networks* (Hungary), 412–417.
- Saadat, S., Buckner, G. D., Furukawa, T., and Noori, M. N. (2003). “Nonlinear system identification of base-excited structures using an intelligent parameter varying (IPV) modeling approach,” in *Proceedings of Smart Structures and Materials, International Society for Optics and Photonics* (San Diego, CA), 555–564.
- Saadat, S., Buckner, G. D., Furukawa, T., and Noori, M. N. (2004a). An intelligent parameter varying (IPV) approach for non-linear system identification of base excited structures. *Int. J. Nonlin. Mech.* 39, 993–1004. doi: 10.1016/S0020-7462(03)00091-X
- Saadat, S., Buckner, G. D., and Noori, M. N. (2007). Structural system identification and damage detection using the intelligent parameter varying technique: an experimental study. *J. Struct. Health Monit.* 6, 231–243. doi: 10.1177/1475921707081980
- Saadat, S., Noori, M. N., Buckner, G. D., Furukawa, T., and Suzuki, Y. (2004b). Structural health monitoring and damage detection using an intelligent parameter varying (IPV) technique. *Int. J. Nonlin. Mech.* 39, 1687–1697. doi: 10.1016/j.ijnonlinmec.2004.03.001
- Sohn, H. (1998). *A Bayesian Probabilistic Approach to Damage Detection for Civil Structures*. Ph.D., Stanford university.
- Soong, T. T., and Spencer, B. F. (2002). Supplemental energy dissipation: state-of-the-art and state-of-the-practice. *Eng. Struct.* 24, 243–259. doi: 10.1016/S0141-0296(01)00092-X
- Spencer, B. F. Jr, and Nagarajaiah, S. (2003). State of the art of structural control. *J. Struct. Eng.* 129, 845–856. doi: 10.1061/(ASCE)0733-9445(2003)129:7(845)
- Wen, Y. K. (1975). Approximate method for nonlinear random vibration. *J. Eng. Mech.* 101, 389–401.
- Wen, Y. K. (1976). Method for random vibration of hysteretic systems. *J. Eng. Mech.* 102, 249–263.
- Wen, Y. K. (1980). Equivalent linearization for hysteretic systems under random excitation. *J. Appl. Mech.* 47, 150–154. doi: 10.1115/1.3153594
- Wen, Y. K. (1986). Stochastic response and damage analysis of inelastic structures. *Probabilist. Eng. Mech.* 1, 49–57. doi: 10.1016/0266-8920(86)90009-3
- Wen, Y. K. (1989). Methods of random vibration for inelastic structures. *J. Appl. Mech. Rev.* 42, 39–52. doi: 10.1115/1.3152420
- Wen, Y. K., and Yeh, C. H. (1989). Biaxial and torsional response of inelastic structures under random excitation. *J. Struct. Saf.* 6, 137–152. doi: 10.1016/0167-4730(89)90016-7
- Worden, K., and Hensman, J. J. (2012). Parameter estimation and model selection for a class of hysteretic systems using Bayesian inference. *Mech. Syst. Signal PR* 32, 153–169. doi: 10.1016/j.ymsp.2012.03.019
- Wu, M., and Smyth, A. W. (2007). Application of the unscented Kalman filter for real-time nonlinear structural system identification. *J. Struct. Control Health Monit.* 14, 971–990. doi: 10.1002/stc.186
- Wu, M., and Smyth, A. W. (2008). Real-time parameter estimation for degrading and pinching hysteretic models. *Int. J. Nonl. Mech.* 43, 822–833. doi: 10.1016/j.ijnonlinmec.2008.05.010
- Yang, J. N., Lin, S., Huang, H., and Zhou, L. (2006). An adaptive extended Kalman filter for structural damage identification. *J. Struct. Control Health Monit.* 13, 849–867. doi: 10.1002/stc.84
- Yuen, K. V., and Katafygiotis, L. S. (2001). Bayesian time-domain approach for modal updating using ambient data. *Probabilist. Eng. Mech.* 16, 219–231. doi: 10.1016/S0266-8920(01)00004-2
- Zadeh, L. (1956). On the identification problem. *IRE Trans Circ. Theory* 3, 277–281. doi: 10.1109/TCT.1956.1086328
- Zhang, B. T., and Cho, D. Y. (2001). System identification using evolutionary Markov Chain Monte Carlo. *J. Syst. Architect.* 47, 587–599. doi: 10.1016/S1383-7621(01)00017-0
- Zhao, Y., Noori, M., and Altabay, W. A. (2017a). Damage detection for a beam under transient excitation via three different algorithms. *J. Struct. Eng. Mech.* 63, 803–817.
- Zhao, Y., Noori, M., Altabay, W. A., and Bahram Beheshti-Aval, B. (2017b). Mode shape based damage identification for a reinforced concrete beam using wavelet coefficient differences and multi-resolution analysis. *J. Struct. Control Health Monitor.* 25, 1–41. doi: 10.1002/stc.2041
- Zhao, Y., Noori, M., Altabay, W. A., and Wu, Z. (2018). Fatigue damage identification for composite pipeline systems using electrical capacitance sensors. *J. Smart Mater. Struct.* 27:8. doi: 10.1088/1361-665X/aacc99
- Zheng, W., and Yu, Y. (2013). Bayesian probabilistic framework for damage identification of steel truss bridges under joint uncertainties. *Adv. Civil Eng.* 2013:307171. doi: 10.1155/2013/307171

Conflict of Interest Statement: The authors declare that the research was conducted in the absence of any commercial or financial relationships that could be construed as a potential conflict of interest.

Copyright © 2019 Zhao, Noori, Altabay and Awad. This is an open-access article distributed under the terms of the Creative Commons Attribution License (CC BY). The use, distribution or reproduction in other forums is permitted, provided the original author(s) and the copyright owner(s) are credited and that the original publication in this journal is cited, in accordance with accepted academic practice. No use, distribution or reproduction is permitted which does not comply with these terms.